

# **Major Project Report**

## **'Linking Structural Brain Imaging Modalities with Behavioural Measures using Multivariate Statistical Analysis'**

### **EE449, EE499**

Under Guidance of

Dr. Krishnan Chemmangat

Assistant Professor

Department of Electrical and Electronics Engineering

NITK Surathkal

Dr Dimitri Van de Ville

Associate Professor

Department of Bioengineering

EPFL, Switzerland



**Submitted by**

Akshay Kumar Jagadish

13EE205

**DEPARTMENT OF ELECTRICAL AND ELECTRONICS ENGINEERING**

**NATIONAL INSTITUTE OF TECHNOLOGY KARNATAKA,  
SURATHKAL**

**P.O: SRINIVASNAGAR, MANGALORE – 575025, KARNATAKA**

## DECLARATION

I hereby *declare* that the Project Work entitled "**Linking Structural Brain Imaging Modalities with Behavioural Measures using Multivariate Statistical Analysis**" which is being submitted to the **National Institute of Technology Karnataka, Surathkal** for the award of the Degree of **Bachelor of Technology** in Electrical and Electronics Engineering is a bonafide *report of the work carried out by me*. The material contained in this Project Work Report has not been submitted to any University or Institution for the award of any degree.

Sr. No.	Register No.	Name	Signature
1	13EE205	Akshay Kumar Jagadish	

Department of Electrical and Electronics Engineering

Place: NITK Surathkal

Date:

## **C E R T I F I C A T E**

This is to certify that the B.Tech. Project Work entitled “Linking Structural Brain Imaging Modalities with Behavioural Measures using Multivariate Statistical Analysis” submitted by:

Sr. No.	Register No.	Name
1	13EE205	Akshay Kumar Jagadish

As the record carried out by him, is *accepted as the B.Tech Project Work Report submission* in partial fulfillments of the requirements for the award of degree of **Bachelor of Technology** in Electrical and Electronics Engineering.

Guide

Dr. Krishnan Chemmangat  
Assistant Professor  
Department of Electrical and Electronics Engineering  
NITK Surathkal

Signature & Date:

Chairman – DUGC  
(Signature with Date & Seal)

A common man with  
uncommon determination  
can change the world.

To my family, friends . . .



## Acknowledgements

I would like thank Summer Research Program – 2016, EPFL for selecting me for the programme. It has truly changed my life. I would like to thank Professor Dimitri Van de Ville for agreeing to supervise me remotely over the period of September to December – 2016 and my team which includes Dr. Djalel Meskaldji (project supervisor), Dr. Sven Haller (Neuro-radiologist) and other fellow lab member at MIP lab. I would like to thank Professor Krishnan CMC for accepting to be my internal project supervisor without whose support it would not been possible to conduct the project and Professor Vinatha, HOD, Electrical Engineering for providing her unstinting support. Last but not the least, my parents and friends for encouraging me to take up this ambitious project at EPFL.



# Abstract

In this work, we investigate the relationship between the principle components of Tract-based Spatial Statistics (TBSS), derived from Fractional Anisotropy (FA) measures, and demographic (Age and Sex), neropsychological and NEO-Personal Inventory (NEOPI) measures. Naturally, Canonical Correlation Analysis (CCA), a multivariate statistical technique, that maximizes the correlation between linear combination of behavioral and imaging features was chosen for the analysis. The CCA modes of correlation so obtained were further tested for statistical significance by performing non-parametric test ( $\alpha = 0.05$ ) and for consistency by Bootstrapping over multiple folds of the data. Thereby, validating the existence of a single, highly significant mode of co-variation that relates (specific region of the brain) with behavioral measures.

Key words: Canonical Correlation Analysis, Fractional Anisotropy, Tract Based Spatial Statistics.



# Contents

<b>Acknowledgements</b>	<b>i</b>
<b>Abstract</b>	<b>iii</b>
<b>Literature Survey</b>	<b>1</b>
<b>1 Brief Introduction to Behavioral Measures</b>	<b>7</b>
1.1 NEO- Personal Inventory (NEOPI-R) . . . . .	7
1.1.1 Facets of NEOPI-R . . . . .	8
1.1.2 Applications Of NEOPI-R . . . . .	8
1.2 Episodic Memory . . . . .	9
1.2.1 Types of Memory Processing . . . . .	9
1.2.2 Anatomy of Episodic Memory . . . . .	11
1.2.3 Quantifying Episodic Memory . . . . .	11
1.2.4 Advantages and Impairments in Episodic Memory . . . . .	11
1.3 Mini-Mental State Examination . . . . .	12
1.3.1 Other Advantages . . . . .	12
<b>2 Structural Brain Imaging - An Introduction</b>	<b>15</b>
2.1 Basic Pre-processing of MR Images . . . . .	15
2.1.1 Bias Field Correction: . . . . .	15
2.1.2 Registration . . . . .	15
2.1.3 Brain Extraction: . . . . .	16
2.1.4 Brain and Tissue-Type Segmentation: . . . . .	16
2.2 Types of Brain Imaging Modalities Used for Analysis . . . . .	17
2.2.1 Arterial Spin Labeled (ASL) Imaging . . . . .	17
2.2.2 3D T1 Image with Accentuated Grey Matter . . . . .	19
2.2.3 Diffusion Tensor Imaging . . . . .	19
2.2.4 Tract-Based Spatial Statistics . . . . .	20
<b>3 Tools Required</b>	<b>23</b>
3.1 Principle Component Analysis - Dimensionality Reduction . . . . .	23
3.2 Canonical Correlation Analysis . . . . .	23
3.2.1 Definition . . . . .	24

## Contents

---

3.3 Hypothesis Testing . . . . .	24
3.3.1 Types of Errors . . . . .	24
3.3.2 Hypothesis Tests and its test statistic . . . . .	25
3.4 Permutation Testing . . . . .	26
3.4.1 Permutation Test . . . . .	27
3.4.2 Considerations . . . . .	28
3.5 Bootstrapping . . . . .	29
3.5.1 Approach . . . . .	29
3.5.2 Illustration . . . . .	29
3.5.3 Discussion . . . . .	30
3.6 Procrustes Analysis . . . . .	31
3.6.1 Algorithm . . . . .	31
3.7 Brain Atlas . . . . .	33
3.7.1 Using the Atlas . . . . .	36
<b>4 Methodology</b>	<b>39</b>
4.1 Data Preparation and Analysis: . . . . .	39
4.1.1 Categorization of Data . . . . .	39
4.1.2 Imaging Data: . . . . .	39
4.1.3 Behavioral Measures: . . . . .	40
4.2 Statistical Testing: . . . . .	40
4.3 Imaging and Behavioral Saliency Vector . . . . .	40
<b>5 Results and Discussion</b>	<b>43</b>
5.1 Arterial Spin Labelled Imaging . . . . .	43
5.2 3D T1 with Accentuated Grey Matter . . . . .	45
5.3 Fractional Anisotropy . . . . .	45
5.4 Tract Based Spatial Statistics . . . . .	47
5.4.1 Pre-processing of Fractional Anisotropy Data . . . . .	47
5.5 Results using TBSS - A Combination of Behaviors Approach . . . . .	49
5.5.1 Stable Controls . . . . .	49
5.5.2 Stable and Deteriorated Controls . . . . .	50
5.6 Results using TBSS - Single Behavioral Analysis . . . . .	50
5.6.1 Stable Controls . . . . .	50
5.6.2 Stable and Deteriorated Controls . . . . .	52
5.6.3 Interpretation using Atlas . . . . .	53
5.7 Finding the structure in each component based on Energy . . . . .	56
<b>6 Conclusion</b>	<b>71</b>
<b>Bibliography</b>	<b>74</b>

# Literature Survey

Anthony et al. in [McIntosh(1999)], were the first to examine the possibility of finding the relation between large-scale neural systems and cognition. Anthony et. al used Partial Least Squares (PLS) and developed a structural equation, in which they confirmed that cognition is governed by interactions with anatomically related regions. A comprehensive framework for understanding neural mechanisms of normal cognition and disease was conducted by Paul et. al [Matthews and Hampshire(2016)]. In which, they focus on application of functional imaging to study a population and draw clinical inferences.

Bratuslav et. al [Bratslav and Sporns(2016)] gave the big picture, in a review, as to how brain connectivity - quantified at multiple levels: from single connections to communities and networks, form the basis for cognitive operations and a diverse repertoire of behaviors. Joshua et. al in [Joshua(2014)] applied unsupervised learning to map ontogenetic (light) stimulation of individual neurons to a set of simple behaviours, such as turning or moving, in animals. The resulting atlas probabilistically relates a large number of individual neurons (embedded in functional circuits) to a set of behavioural types. By extending the use machine learning-based techniques, Miranda et. al [Miranda(2014)] use connectivity patterns to identify individuals, called as 'connectotyping', where a approach for characterizing resting state functional connectivity MRI (fcMRI) was designed, that acts as a functional finger print of individual participant.

Recently, Smith in [Smith and Nichols(2015)] found the relationship between individual subjects' (of a total 461 ) functional connectomes [Sporns(2014)] and 280 behavioral and demographic measures, in a single holistic analysis. We delve deeper into the work as it form the crux of the research conducted. Smith et al. examined the SMs most strongly associated (positively or negatively) with the identified CCA mode (Fig. 1a and Supplementary Table 1), as well as the relationships of all subjects with this mode (Fig. 1b), that is, individual subject scores in the SM canonical variate versus subject scores in the connectome canonical variate (one point per subject). This mode of population co-variation resembles descriptions of a general intelligence g factor, but extends it to include key aspects of real-life function, including years of education, income and life satisfaction. This can be considered a one-dimensional positive-negative axis, insofar as nearly all the positively correlated SMs are commonly considered as positive personal qualities or indicators (for example, high performance on memory and cognitive tests, life satisfaction, years of education, income), and all negatively correlated SMs

## Contents

---

relate to negative traits (for example, those related to substance use, rule-breaking behavior, anger). One notable example is the strongly negative position of cannabis usage on the scale (although this is not on its own driving the overall results, which are almost unchanged if cannabis users are excluded from the CCA; Online Methods). High-scoring subjects (top-right points in the scatter plot) have high relative values for positive SMs (at the top of the SM list) and low relative values for negative SMs (at the bottom). In low-scoring subjects (bottom-left points), the pattern is reversed, with high values for negative SMs and low values for positive ones.

They next investigated whether this one CCA mode is indeed unique in modeling a substantially larger fraction of the total population variance (in the connectome and SM matrices) than the other 99 modes estimated. It is clear (Fig. 1c) that the first CCA mode explains a much larger fraction of the total data than any other mode and is the only one to fall far outside the null confidence interval. Using the null distributions to normalize the variance explained into z scores, they found that the primary CCA mode has  $Z = 7.7$  for connectomes (the largest of any of the other 99 modes is 2.7) and  $Z = 9.2$  for SMs (the largest of any other mode is 2.4). Figure 2a displays the brain connections most strongly associated with the CCA mode. There was positive overall correlation (across edges,  $r = 0.20$ ) between the CCA connectome-modulation weights and the original population mean connectome, indicating that subjects that score highly in this CCA mode have stronger connectivity overall than low-scoring subjects.

When the data are summarized according to brain regions that most strongly contribute to these connections, a pattern emerges (Fig. 2b) that includes bilaterally symmetric peaks in medial frontal and parietal cortex, in the temporo-parietal junction and in anterior insula and frontal operculum. These regions, taken together, have high spatial overlap with the default mode network. Although precise anatomical dissociations and functional specializations among these regions is the subject of debate in cognitive neuroscience, they have been associated with many higher level aspects of human cognition, including episodic and semantic memory, imagination and construction, value-guided decision-making, delay discounting, spatial reasoning, and high-order social process such as theory of mind. With deference to the caution required when making reverse inferences, it may be expected that these aspects of cognitive function would have an influence on life in a complex society. Although there are peaks in dorsal prefrontal cortex, it is notable that the highest node strengths are not centered on the dorsolateral prefrontal regions often associated with fluid intelligence.

In summary, they found one significant mode of population variation that links a specific pattern of brain connectivity to a specific pattern of covariance between many behavioral and demographic subject measures. The vast majority of the SMs that correlate positively with this mode are positive subject traits and measures (education, income, IQ, life-satisfaction); those that correlate negatively are mostly negative subject measures. However, although it strongly resembled the known general intelligence g factor for many of the subject measures, this mode did not trivially map onto just the strongest single principal component of the subject measures; the CCA mode mapped strongly onto the top three SM principal components and

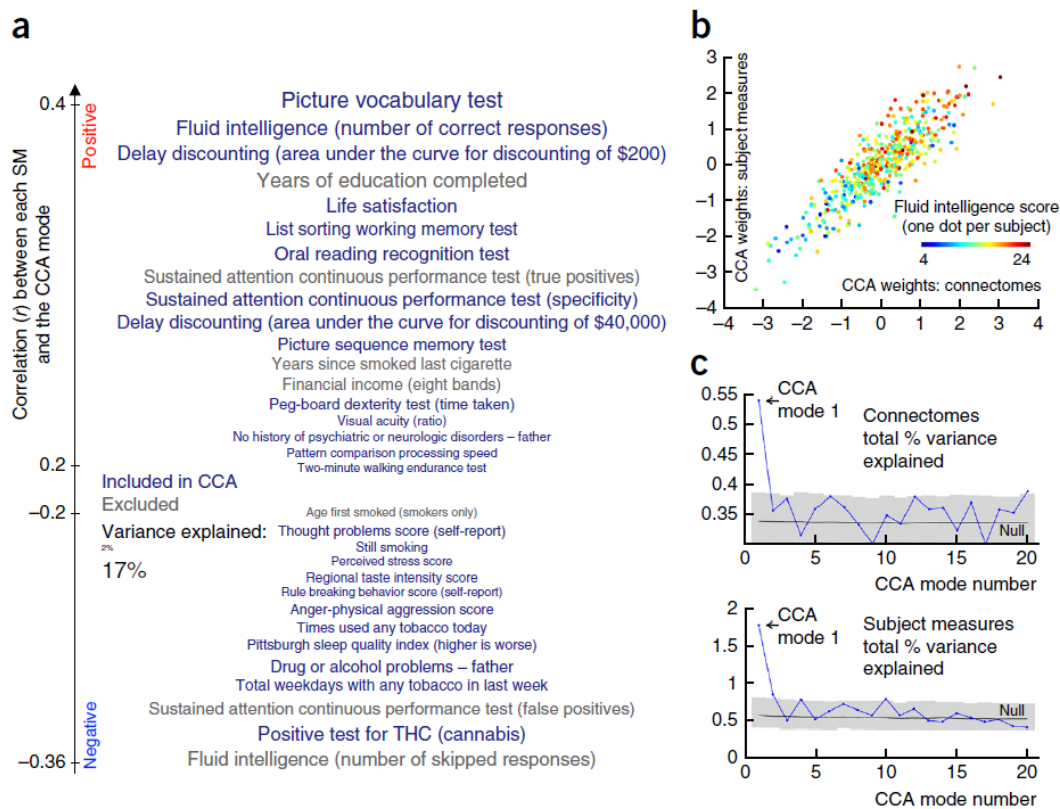


Figure 1 – CCA mode subject measure weights, connectome weights and data variance explained.(a) The set of SMs most strongly associated with the CCA mode of population variability. SMs included in the CCA are colored blue, whereas others (gray) were correlated with the CCA mode post hoc. Vertical position is according to correlation with the CCA mode and font size indicates SM variance explained by the CCA mode. We do not report 'secondary' SMs that are highly redundant with those shown here (Supplementary Table 1 shows the complete set of SMs that correlate highly with the CCA mode) (b) The principal CCA mode, a scatter plot of SM weights versus connectome weights, with one point per subject, and an example subject measure (fluid intelligence) indicated with different colors. The high correlation visualized here indicates significant co-variation between the two data sets. (c) The total variance explained of the original data matrices (shown separately for connectomes and subject measures) is plotted for the first 20 CCA modes. The mean and the 5th to 95th percentiles of the null distribution of the same measures, estimated via permutation testing, are shown in black and gray. Using the null distributions to normalize variance explained accounts for the fact that the initial modes are expected to have higher correlations, even in the null scenario, but, as can be seen from the nulls, this is a very small effect in any case.

## Contents

---

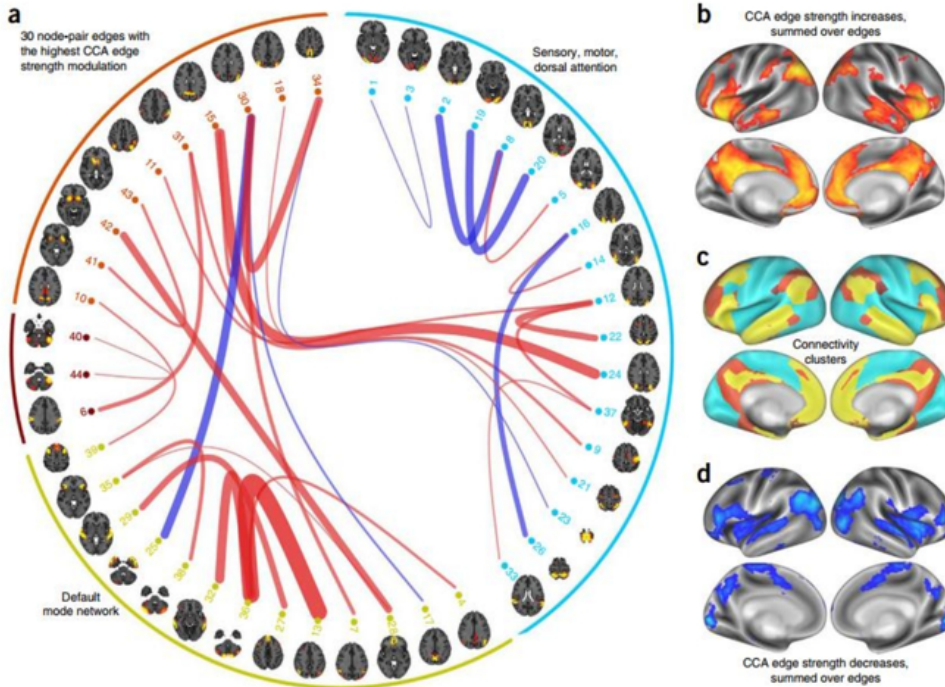


Figure 2 – CCA mode connectome weights and associated spatial maps. (a) The 30 brain connections most strongly associated with the CCA mode of population variability. To aid interpretation, the CCA edge modulation weights are multiplied by the sign of the population mean correlation; hence red indicates stronger connections and blue weaker, for high-scoring subjects (and vice versa for low-scoring subjects). (b) Map of CCA connection strength increases (each node's parcel map is weighted by CCA edge-strength increases, summed across edges involving the node). (c) Group-mean functional clustering: four clusters from a hierarchical analysis of all 200 nodes' population-average full correlation (Supplementary Fig. 3). These fall into two groups: one cluster (blue) contains sensory, motor, insula and dorsal attention regions, and a group of three correlated clusters (brown, red, yellow) primarily covering the default mode network and subcortical/cerebellar regions. (d) Data presented as in b, but showing CCA connection strength decreases. Maps in d and b are largely non-overlapping except in insula. Map in b has spatial correlation of +0.40 with the default-mode areas shown in c (that is, high overlap), whereas the map in d has negative correlation (-0.12). The average connectivity strength increase was approximately double that of the average decrease (as reflected in the predominance of red edges in a; also, a single map averaging across all 200 edges for each node showed a pattern of overall increase highly similar to that in b; finally, both the maps in b and d were thresholded at the 80th percentile of their respective distributions, and if the threshold applied to b were applied to d, none of the strength reductions shown would survive).

not just the first). It is plausible that the CCA mode includes a neural correlate of  $g$ , but is a more general mode of positive brain function and is more directly tied to the underlying biology (specifically, connectivity between brain regions), given that it is driven both by structured population covariance in behavioral measures and by intrinsic brain connectivity.

However, all the aforementioned works link functional connectivity networks with behavior and cognition. Thereby, opening doors for analysis of structural connectivity networks or structural population covariance maps so as to link them to neuropsychological scores.



# **1 Brief Introduction to Behavioral Measures**

## **1.1 NEO- Personal Inventory (NEOPI-R)**

The Revised NEO Personality Inventory (NEO-PI-R) is a cutting-edge instrument. The research on neuroticism, extraversion, and openness to experience began in the mid-1970s, but already by 1983, they had begun to add measures of agreeableness and conscientiousness. Research has continued since publication of the NEO-PI in 1985, resulting in a manual supplement issued in 1989 and a major revision introducing facet scales for agreeableness and conscientiousness in 1992. Item changes to improve internal consistency and readability led to the NEO-PI-3. As of now, the NEO-PI-R inventory incorporates the latest advances in personality structure and assessment; the 'neo' in the title is an intended pun. In other respects, the NEO-PI-R is profoundly conservative, deeply rooted in the research of generations of personality psychologists. Most of the traits it measures have long been familiar, and scale labels have been chosen to emphasize continuity with past conceptualizations. The psychometric strategies for item selection and scale validation has been benefited from the insight and experience of many previous researchers and theorists. Thereby, taking on the onus of carrying the traditions of personal assessment.

The transition from "three-factor" to current "five-factor" model started off with the three factors namely, neuroticism (N), extraversion (E), and openness (O). The first two factors were common in analyses of the 16PF (as anxiety and 'exvia'); and, in addition, clearly corresponded to the major dimensions of Eysenck's system. However, the third dimension made it possible for the Costa et al. to go a step beyond Eysenck's work, and identify a new fundamental dimension [McCrae and Costa(1986)]. Rather than adopting the factor-analytic language of first-order and second-order factors, N, E, and O adopted broad domains of traits, and were more specific traits as their facets [McCrae and John(1992)].

The approach in designing the model was to measure each domain by summing scores on a half-dozen facet scales. The user would thus have highly reliable measures of three global domains, as well as more specific information on traits within each domain. The resulting questionnaire was the NEO Inventory.

## **Chapter 1. Brief Introduction to Behavioral Measures**

---

**Table 1.1 – Personality Facets Measurement**

Neuroticism	Extraversion	Openness to experience	Agreeableness	Conscientiousness
Anxiety	Warmth	Fantasy	Trust	Competence
Hostility	Gregariousness	Aesthetics	Straightforwardness	Order
Depression	Assertiveness	Feelings	Altruism	Dutifulness
Self-consciousness	Activity	Actions	Compliance	Achievement Striving
Impulsiveness	Excitement Seeking	Ideas	Modesty	Self-Discipline
Vulnerability to Stress	Positive Emotion	Values	Tendermindedness	Deliberation

Research using the aforementioned instrument showed the utility of the three-dimensional model in understanding phenomena such as somatic complaints, psychological well being , ego development, and vocational interests. The validity of the scales themselves was demonstrated by convergence with other instruments. The three domains of N, E, and O were clearly central variables in personality psychology, but they were just as clearly incapable of addressing the full range of individual differences. But the approach was strengthened by researchers from different fields like Norman, in 1963, reinforced it by identifying similar dimensions called extraversion or surgency, agreeableness, conscientiousness, emotional stability, and culture. This newly proposed five-factor model appeared to provide a robust and comprehensive description of the natural language of traits, if not traits themselves. It was clear that Norman's extraversion strongly resembled NEO-PI's extraversion, and that emotional stability propounded was the polar opposite of N. There was some suggestion that culture was a variant of O. An empirical test confirmed these hypotheses and also pointed to the importance of agreeableness (A) and conscientiousness (C), domains unrepresented in the NEO Inventory. Therefore, brief scales to measure these two domains were constructed and published the final instrument as the NEO Personality Inventory.

A series of subsequent analyses showed that the five- factor model operationalized by the NEO-PI was in fact extraordinarily comprehensive: It encompassed dimensions in Murray's needs [Costa and McCrae(1988)]; the interpersonal circumplex ; Jungian typologies ; and the items of Block's (1961) California Adult Q-Set [McCrae and John(1992)]. But it had a major limitation, the facets of A and C were yet to be discovered. Then, on conducting item selection and facet validation studies in several samples [McCrae and John(1992)], the Revised NEO Personality Inventory (NEO-PI-R) was published in 1992.

### **1.1.1 Facets of NEOPI-R**

The table 1.1 of the personality dimensions measured by the NEOPI-R, including facets, is as follows:

### **1.1.2 Applications Of NEOPI-R**

The appeal of the model is threefold: It integrates a wide array of personality constructs, thus facilitating communication among researchers of many different orientations; it is compe-

hensive, giving a basis for systematic exploration of the relations between personality and other phenomena; and it is efficient, providing at least a global description of personality with as few as five scores. Of these, comprehensiveness is perhaps the most crucial. Without a comprehensive model, studies using personality traits as predictors are inconclusive, because the most relevant traits may have been overlooked. This is unlikely to happen when measures of all five factors are included in a study. Indeed, even null results are informative in such a study: If none of the factors is related to the criterion, it may be time to abandon the search for personality predictors.

The Five-factor model has been found to be profitably used in most applied settings. It has found its feet in education, industry, forensic and health care sectors. Further it can also be used in evaluating other neuropsychological scales and also for self understanding by performing the test on oneself.

## **1.2 Episodic Memory**

Episodic memory [Tulving and Markowitz(1998)] refers to the memory of an event or episode. Episodic memories allow us to mentally travel back in time to an event from the recent or distant past (remote memories). Episodic memories include various details about these events, such as what happened, when it happened and where it happened. To help understand this concept, try to remember the last time you ate dinner at a restaurant. The ability to remember where you ate, who you were with and the items you ordered are all features of an episodic memory. Other examples of episodic memory include remembering where you parked your car this morning or the more remote memory of where you were when you heard about the September 11th attacks. Episodic memory is typically thought to fall under the larger umbrella of declarative memory, meaning that episodic memories can be explicitly or consciously recalled. However, studies have suggested that details of episodic memories can be recognized even without conscious recollection of the event.

Episodic memory is distinct from another type of declarative memory called semantic memory. Semantic memory refers to your fund of general knowledge. To build upon a previous example, remembering where you parked your car is an example of episodic memory; your general knowledge and concepts about what a car is and how an engine works are examples of semantic memory. Episodic and semantic memory are each related to different systems in the brain, although they are often considered to be functionally related. Episodic memory can be thought of as a process with several different steps, each of which relies on a separate system of the brain.

### **1.2.1 Types of Memory Processing**

The recollection of experiences is contingent on three steps of memory processing:

1. Encoding

## **Chapter 1. Brief Introduction to Behavioral Measures**

---

2. Consolidation/storage
3. Retrieval.

### **Encoding**

The initial step in forming an episodic memory is called encoding, which is the process of receiving and registering information. Encoding is necessary for creating memory representations of information or events that you experience. The process of encoding is dependent on the degree that you attend to an event or information. That is, if you are not attending to an event while it is happening because you are distracted, then you are less likely to remember the details from the event. Attention is a necessary component for effectively encoding events or information. Encoding of episodic memories is also influenced by how you process the event. Encoding of information can be strengthened by an "elaboration process", which can involve making connections between the information at hand or relating the information to your personal experiences. For example, if you were asked to remember and buy 10 items at the grocery store, you would likely remember more of the items if you used a strategy of making a mental connection between the items rather than if you were to simply repeat the items a couple of times.

### **Consolidation**

Memory consolidation, the next step in forming an episodic memory, is the process by which memory traces of encoded information are strengthened, stabilized and stored to facilitate later retrieval. Consolidation is most effective when the information being stored can be linked to an existing network of information. It is also strengthened by repeated access of the information to be remembered. The neural pathways from the hippocampus to the cortex underlie the process of consolidation and storage. The number of neurons that are dedicated to a particular memory, as well as the frequency with which they fire together, help to strengthen the memory traces within the cortex. This process of consolidation occurs over the course of days to weeks and is subject to reorganization when new, relevant information is learned.

### **Retrieval**

The last step in forming episodic memories is called retrieval, which is the conscious recollection of information that was encoded. Retrieving information from episodic memory depends upon contextual information or cues and whether the information was encoded and stored into memory. Thus, if the information was not properly encoded because you were distracted, you may be less likely to remember details of the event or information. Emotional, semantic knowledge, olfactory, auditory and visual factors can act as cues or contextual information to help in the retrieval of episodic memory. For example, when recalling where you parked your

car you may use the color of a sign you parked near and/or the floor of the parking structure as cues.

### **1.2.2 Anatomy of Episodic Memory**

One way in which we learn about the function of brain structures is by studying the effect of damage to these structures. Our current understanding of the anatomy of episodic memory was influenced by the study of epilepsy patient H.M. who underwent resection, or surgical removal, of the hippocampus and surrounding structures. The hippocampus, named after its resemblance to a seahorse, is a brain structure located in the inner (medial) temporal lobe. Following this surgery to reduce his seizures, he was no longer able to form new memories, implicating the hippocampus in episodic memory. Further studies have confirmed the role of the hippocampus and surrounding structures in episodic memory.

However, the hippocampus does not function in isolation, but rather works in harmony with a network of other brain areas. One important network, referred to as the default mode network, includes several brain areas including frontal and parietal regions. The default mode network has been implicated in episodic memory functioning. The hippocampus, its surrounding regions and the default mode network are susceptible to many types of neurological insults. One particular type of insult commonly seen in older adults is Alzheimer's disease. Alzheimer's disease pathology most often originates in medial temporal structures including the hippocampus and is known to affect default mode network connectivity. Indeed, episodic memory impairment is a hallmark sign of Alzheimer's disease. In addition to the hippocampus and default mode network, other brain structures that play a role in episodic memory are the thalamus, mammillary bodies and the amygdala. The brain regions associated in the default network can become activated when examining the different processes involved in episodic memory. In the brain, PET and fMRI studies have found that episodic retrieval is associated with activation in the right prefrontal cortex.

### **1.2.3 Quantifying Episodic Memory**

A common way to assess episodic memory is by using neuropsychological tests, including pen-and-paper, verbal and computer-based tasks. These measures give a clinician an objective method for evaluating how well a patient's episodic memory is functioning compared to their peers. Asking an examinee to remember a list of words or recall a story are common methods for assessing verbal episodic memory

### **1.2.4 Advantages and Impairments in Episodic Memory**

It is extremely important to study and measure episodic memory in our case since it is affected early in the course of dementia. Which might eventually lead to a neurogenerative disease such as Alzheimer's disease. But there are a wide range of neurologic diseases and conditions

## **Chapter 1. Brief Introduction to Behavioral Measures**

---

that can affect episodic memory. These include, but are not limited to subarachnoid hemorrhage, trauma, hydrocephalus, tumors, metabolic conditions including vitamin B1 deficiency, infectious and inflammatory conditions such as Hashimoto's encephalopathy.

### **1.3 Mini-Mental State Examination**

The Mini-Mental State Examination (MMSE), as developed by Folstein, Folstein, and McHugh [Folstein(1975)], is the most widely used of cognitive screening tools. It is used to test for complaints of problems with memory or other mental abilities. It can be used by clinicians to help diagnose dementia and to help assess its progression and severity. It consists of a series of questions and tests, each of which scores points if answered correctly. Some of the questions in the questionnaire are as follows:

The MMSE tests a number of different mental abilities, including a person's memory, attention and language. Also, it is only one part of assessment for dementia. Clinicians will consider a person's MMSE score alongside their history, symptoms, a physical exam and the results of other tests, possibly including brain scans. Further, MMSE can also be used to assess changes in a person who has already been diagnosed with dementia. It can help to give an indication of how severe a person's symptoms are and how quickly their dementia is progressing. Again, results should be considered alongside other measures of how the person is coping together with clinical judgement.

MMSE is reliable on 24 hour or 28 day retest by single or multiple examiners. When the Mini-Mental status was given twice, 24 hour apart by the same tester on both occasions, the correlation by Pearson coefficient was 0.887. If the aforementioned is repeated with a different examiner, the correlation was found to be 0.827. Thus, the scores seem stable even when multiplex examiners are used. When elderly depressed and demented patients chosen for their clinical stability were given the Mini-Mental Status twice, an average of 28 days apart, there was no significant difference in these scores and the product moment correlation for test 1 vs test 2 was 0.98.

#### **1.3.1 Other Advantages**

1. It is a valid test of cognitive function. It separates patients with cognitive disturbance from those without such disturbance. Its scores follow the changes in cognitive state when and if patients recover.
2. Given that it is a quantified assessment of cognitive state of demonstrable reliability and validity, it makes more objective what is commonly vague and subjective impression of cognitive disability.
3. It can be repeated during an illness and shows little practical effect. Making it suitable for initial and serial measurements of cognitive function, and can demonstrate worsening

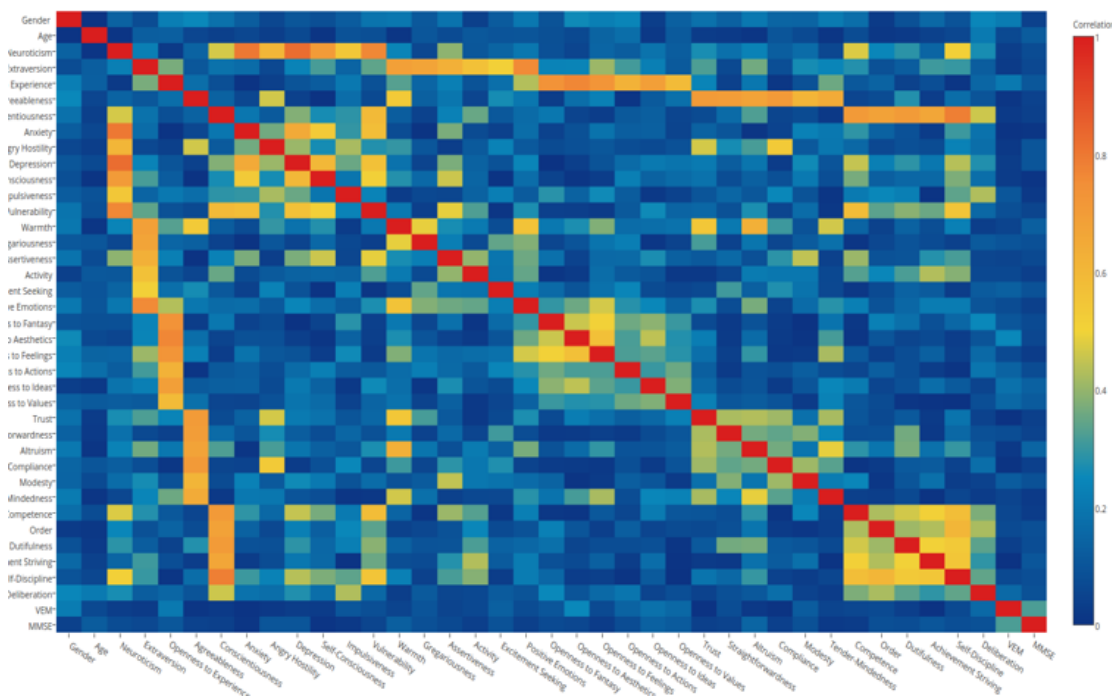


Figure 1.1 – Correlation Matrix of NEOPI Measures

or improvement of the feature over time and with treatment.

4. The implications from the MMSE score are easily appreciated by other professionals such as lawyers, judges and social workers concerned with such issues as the patient's competency to manage his daily affairs. It can therefore aid in bringing to the patient the social supports that he needs.
5. It is found to be useful in teaching psychiatric residents to become skillful in evaluation of the cognitive aspects of the mental status. It provided them with a standard set of questions instead of bombarding the patients with individual set of questions.

In Figure 1.1, we visualize the correlation matrix taking into account the 37 behavioral metrics under our disposal - 5 (NEOPI) + 6\*5 (NEOPI Subscores) + 2 (MMSE + VEM) and demographic measures - Age and Gender. It can be observed that the 6 subscores of a given NEOPI measure are correlated to one another. However, it can also be seen that there are few subscores belonging to other NEOPI measure that is also correlated with a given subscore indicating that these subscores are not mutually exclusive of one another. Instead as discussed earlier the scores are selected such that most amount of information is encompassed and not making each measure independent of each other.



## **2 Structural Brain Imaging - An Introduction**

### **2.1 Basic Pre-processing of MR Images**

#### **2.1.1 Bias Field Correction:**

The bias field, also called the intensity inhomogeneity, is a low-frequency spatially varying MRI artifact causing a smooth signal intensity variation within tissue of the same physical properties; see Figure 6. The bias field arises from spatial inhomogeneity of the magnetic field, variations in the sensitivity of the reception coil, and the interaction between the magnetic field and the human body. The bias field is dependent on the strength of the magnetic field. When MR images are scanned at 0.5 T, the bias field is almost invisible and can be neglected. However, when MR images are acquired with modern high-field MR scanners with a magnetic field strength of 1.5 T, 3 T, or higher, the bias field is strong enough to cause problems and considerably affect MRI analysis. Therefore, the correction of the bias field is an important step for the efficient segmentation and registration of brain MRI.

#### **2.1.2 Registration**

Image registration is the process of overlaying (spatially aligning) two or more images of the same content taken at different times, from different viewpoints, and/or by different sensors. Registration is required in medical image analysis for obtaining more complete information about the patient's health when using multimodal images (e.g., MRI, CT, PET, and SPECT) and for treatment verification by comparison of pre- and post intervention images. In medical image registration the term coregistration is used for intrasubject registration (the alignment of multimodal images of the same subject), realignment is used for motion correction within the same subject, and normalization is used for intersubject registration when several population groups are studied.

It involves finding the transformation between images so that corresponding image features are spatially aligned. The spatial alignment is typically initialized using rigid or affine transfor-

mation. A rigid transformation is a 6-parameter transformation composed of translation and rotation. If scaling and skewing are allowed, we obtain a 12-parameter affine transformation. A rigid registration is sufficient for intrasubject registration if the object of interest does not deform. This is a reasonable assumption for images of the brain if these are acquired at the same stage of brain development. However, if the task is to match images belonging to either different subjects (intersubject registration) or the same subject at different stages of brain development (e.g., growth in children, changes related to ageing, or atrophy due to disease), a nonrigid registration of the images is required to obtain satisfactory results. The nonrigid registration algorithms are typically based on either physical models for transformation such as elastic or fluid deformation models or a linear combination of smooth basis functions or free-form deformations.

### **2.1.3 Brain Extraction:**

Nonbrain tissues such as fat, skull, or neck have intensities overlapping with intensities of brain tissues. Further, these surrounding tissues and acquisition artefacts can hamper the subsequent data-processing. Therefore, the brain has to be extracted before brain segmentation methods can be used. This step classifies voxels as brain or nonbrain. The result can be either a new image with just brain voxels or a binary mask, which has a value of 1 for brain voxels and 0 for the rest of tissues. The scalp, dura matter, fat, skin, muscles, eyes, and bones are always classified as nonbrain voxels.

The current best method for extracting the brain is the brain extraction tool (BET), which is part of the publicly available software package FSL. This method finds the center of gravity of the brain and then inflates a sphere until the brain boundary is found. It has been proven to work in practice on good quality T1-W and T2-W images of the adult brain. However, for functional image which provides little non-brain tissue, brain extraction is performed using FEAT and MELODIC.

### **2.1.4 Brain and Tissue-Type Segmentation:**

The brain MRI segmentation is an essential part for many clinical applications because it influences the outcome of the entire analysis. Its fundamental components in structural brain MRI analysis include the classification of MRI data into specific tissue types and the identification and description of specific anatomical structures. The segmentation methods, with application to brain MRI, may be grouped as follows:

- (i) manual segmentation;
- (ii) intensity-based methods;
- (iii) atlas-based methods;
- (iv) surface-based methods (including active contours and surfaces, and multiphase active contours);
- (v) hybrid segmentation methods.

## **2.2. Types of Brain Imaging Modalities Used for Analysis**

---

In this work, however, the intensity-based method was used. Where segmentation is performed purely on the basis of voxel intensity, once intensity thresholds have been found to optimally distinguish between the different tissue classes. This can be considered as an analysis of the image histogram, where the different classes appear (ideally) as separate peaks, which have a spread caused by factors such as image noise, motion artefacts, partial-volume effect, bias field (intensity fluctuations across the image caused by inhomogeneities in the radio-frequency field) and true within-class variation.

## **2.2 Types of Brain Imaging Modalities Used for Analysis**

In our case, three modalities were extracted for each of the 377 subjects - stable controls, deteriorated Controls and Mild Cognitive Impairment (MCI). The three modalities are Arterial Spin Labeled Imaging (ASL), 3D T1 Imaging with Accentuated Grey Matter and Diffusion Tensor Imaging. Each of them have been elaborated below.

### **2.2.1 Arterial Spin Labeled (ASL) Imaging**

Arterial spin labeling (ASL) [Petcharunpaisa(2010)] is a magnetic resonance imaging technique for measuring tissue perfusion using a freely diffusible intrinsic tracer. Where Perfusion refers to the delivery of oxygen and nutrients to tissue by means of blood flow. As compared with other perfusion techniques, ASL offers several advantages and is now available for routine clinical practice in many institutions. Its noninvasive nature and ability to quan titatively measure tissue perfusion make ASL ideal for research and clinical studies.

Ideally, scientists would like to directly measure neural activity. And is considered a holy grail in medical research. However, as this is nearly impossible under the normal circumstances, most researchers have chosen to observe the changes in the metabolic activity that follow mental work using techniques such as BOLD. Though measuring changes in blood flow as a consequence of neural activity would be the next most direct approach, this was formerly only obtainable through the use of invasive imaging techniques utilizing exogenous radioactive agents. Thus, initially researchers opted to use the BOLD technique, which though dependent on cerebral bood flow (CBF), does not give a direct measure of it. However, with recent advances in MR imaging it is possible to extract CBF measurements non-invasively; It is through ASL.

Prior to ASL, the technique used for determining CBF involved use of exogenous contrast agents (like  $^{15}OH_2O$  radiotracer) in Positron Emission Tomography (PET), single-photon emsission computed tomography (SPECT), CT perfusion and dynamic susceptibility contrast (DSC) MR imaging . In PET technique, researchers inject a radiotracer into the participant and it would then circulate through the body's vascular system, ultimately diffusing freely into brain tissue along with the blood. The radioactive tracer would begin to decay almost immediately, emitting tiny positively charged particles (called positron) which could then be

## **Chapter 2. Structural Brain Imaging - An Introduction**

---

detected using specialized equipment. As the radiotracer travels with the blood, the amount of radioactivity detected reflects blood flow. That is to say, areas which received a lot of blood tend to give higher activity due to higher emissions of radioactive positrons. Thus, in each region of the brain, uptake of radiotracer is proportional to blood flow. but due to this agent it is invasive. Hence, ASL that works on same principle but uses magnetically labeled water, instead of radioactively labeled water, is preferred.

To explain the working of ASL in detail, it is similar to PET technique but with a different kind of tracer. In ASL, the arterial blood water is magnetically labeled then imaged. First, arterial blood water is magnetically labeled just below the region (slice) by applying a radio-frequency (RF) inversion pulse. The result of this pulse is inversion of the net magnetization of the blood water. In other words, the water molecules within the arterial blood are labeled magnetically. After a period of time (called transit time), this 'paramagnetic (temporarily magnetic) tracer' flows into slice of interest where it exchanges with tissue water. The in flowing inverted spins within the blood water alter total tissue magnetization, reducing it and, consequently, the MR signal and image intensity. During this time, an image is taken (called tag image). The experiment is then repeated without labeling the arterial blood to create another image (called the control image). The control image and the tag image are subtracted to produce a perfusion image. This image will reflect the amount of arterial blood delivered to each voxel within the slice within the transit time.

Currently there are four types of ASL techniques that differ, mainly according to the magnetic labeling process - Continuous ASL, CASL, was the very first implementation of ASL, then Pseudo- continuous ASL (PCASL), PASL and velocity-selective ASL (VS-ASL) were developed to address limitations and technical challenges encountered in the first ASL methods.

### **Clinical applications:**

1. Physiological Regional Hyper-fusion: Regional increased signal intensity can occur in both occipital lobes corresponding to visual cortex activation.
2. Age-dependent variability of cerebral perfusion: ASL can demonstrate age dependent cerebral perfusion if a quantitative measurement is used. In pediatric patients undergoing ASL, a consistent pattern of increased SNR, as well as globally elevated absolute CBF, has been observed compared with adults. This is possibly because there is a pediatric higher baseline CBF, faster mean transit time, and increased T1 values in blood and tissue. Pediatric CBF measurements begin at a low level in the perinatal period, increase to a peak at 3-8 years of age and then gradually decrease to adult levels.
3. Cerebrovascular diseases One of the most frequent clinical applications of perfusion imaging is the evaluation of cerebrovascular diseases. Decreased cerebral perfusion is the common underlying cause of all ischemic strokes and is a predictor of recurrent stroke. The perfusion-diffusion mismatch concept is widely used in MR imaging for ischemic acute stroke. Potentially salvageable tissue by timely reperfusion (tissue at risk) can be identified by perfusion imaging.
4. Dementia and cognitive disorders In cognitive disorders, imaging modalities are becoming

## **2.2. Types of Brain Imaging Modalities Used for Analysis**

---

increasingly important for differential diagnosis, for monitoring disease progression, and as surrogate markers in treatment trials studies have demonstrated the ability of ASL in detecting regional hypoperfusion in frontotemporal dementia (FTD), Alzheimer's disease (AD), and mild cognitive impairment (MCI), consistent with previous PET and SPECT studies.

### **Preprocessing Steps involved**

- 1) Outlier detection/ Intra-scan quality control
- 2) Motion correction
- 3) Image denoising-deblurring
- 4) Smoothing
- 5) Coregistration
- 6) EPI distortion correction

### **2.2.2 3D T1 Image with Accentuated Grey Matter**

Using the T1 Image that is acquired after performing aforementioned preprocessing steps, the gray matter is accentuated. First, the images acquired are smoothed by convolving with an isotropic Gaussian kernel. This makes the subsequent voxel-by-voxel analysis comparable to a region of interest approach, because each voxel in the smoothed images contains the average concentration of gray matter from around the voxel (where the region around the voxel is defined by the form of the smoothing kernel). This is often referred to as "gray matter density," but should not be confused with cell packing density measured cytoarchitectonically. By the central limit theorem, smoothing also has the effect of rendering the data more normally distributed, increasing the validity of parametric statistical tests. The size of the smoothing kernel is generally tried to made be comparable to the size of the expected regional differences between the groups of brains. The smoothing step also helps to compensate for the inexact nature of the spatial normalization.

### **2.2.3 Diffusion Tensor Imaging**

Diffusion tensor imaging (DTI)[Le Bihan(2001)] is a magnetic resonance imaging technique that enables the measurement of the restricted diffusion of water in tissue in order to produce neural tract images instead of using this data solely for the purpose of assigning contrast or colors to pixels in a cross sectional image. It also provides useful structural information about muscle—including heart muscle—as well as other tissues such as the prostate.

In DTI, each voxel has one or more pairs of parameters: a rate of diffusion and a preferred direction of diffusion—described in terms of three-dimensional space—for which that parameter is valid. The properties of each voxel of a single DTI image is usually calculated by vector

or tensor math from six or more different diffusion weighted acquisitions, each obtained with a different orientation of the diffusion sensitizing gradients. In some methods, hundreds of measurements—each making up a complete image—are made to generate a single resulting calculated image data set. The higher information content of a DTI voxel makes it extremely sensitive to subtle pathology in the brain. In addition the directional information can be exploited at a higher level of structure to select and follow neural tracts through the brain—a process called tractography.

A more precise statement of the image acquisition process is that the image-intensities at each position are attenuated, depending on the strength ( $b$ -value) and direction of the so-called magnetic diffusion gradient, as well as on the local microstructure in which the water molecules diffuse. The more attenuated the image is at a given position, the greater diffusion there is in the direction of the diffusion gradient. In order to measure the tissue's complete diffusion profile, one needs to repeat the MR scans, applying different directions (and possibly strengths) of the diffusion gradient for each scan.

Given these development, there has been much interest in using magnetic resonance diffusion imaging to provide information about anatomical connectivity in the brain, by measuring the anisotropic diffusion of water in white matter tracts. One of the measures most commonly derived from diffusion data is fractional anisotropy (FA), which quantifies how strongly directional the local tract structure is. Many imaging studies are starting to use FA images in voxelwise statistical analyses, in order to localise brain changes related to development, degeneration and disease. However, optimal analysis is compromised by the use of standard registration algorithms; there has not to date been a satisfactory solution to the question of how to align FA images from multiple subjects in a way that allows for valid conclusions to be drawn from the subsequent voxelwise analysis. Furthermore, the arbitrariness of the choice of spatial smoothing extent has not yet been resolved.

Thus, to address these issues Smith et al. [Smith(2006)] present a new method that aims to solve these issues via (a) carefully tuned non-linear registration, followed by (b) projection onto an alignment-invariant tract representation (the mean FA skeleton). This approach known as Tract-Based Spatial Statistics (TBSS) was used given its ability to improve the sensitivity, objectivity and interpretability of analysis of multi-subject diffusion imaging studies.

### 2.2.4 Tract-Based Spatial Statistics

Magnetic resonance diffusion tensor imaging (DTI) is sensitive to water diffusion characteristics (such as the principal diffusion direction and the diffusion anisotropy) and has therefore been developed as a tool for investigating the local properties of brain tissues such as white matter tracts [Le Bihan, 2003]. There has also been a great deal of interest in using diffusion anisotropy as a marker for white matter tract integrity, for example, for disease diagnosis, tracking disease progression, finding disease sub-categories, studying normal development/aging, and as complementary information to investigating normal brain function. Diffusion

## **2.2. Types of Brain Imaging Modalities Used for Analysis**

---

anisotropy describes how variable the diffusion is in different directions and is most commonly quantified via a measure known as fractional anisotropy (FA). It is highest in major white matter tracts (maximum theoretical value 1) and lower in grey matter while approaching 0 in cerebrospinal fluid. As a marker for tract integrity, FA is a useful quantity to compare across subjects as it is computable voxelwise and is a scalar value that is independent of the local fibre orientation (and therefore a relatively objective and straightforward measure to compare across subjects). There has been much debate about the strengths and limitations of VBM [Bookstein, 2001; Ashburner and Friston, 2001; Davatzikos, 2004; Ashburner and Friston, 2004]. Some researchers continue to doubt the general interpretability of the results from this approach, primarily because there can be ambiguity as to whether apparent changes are really due to change in grey matter density or simply due to local misalignment, though it does seem that through careful application and validation, structural imaging studies using VBM can draw valid conclusions (e.g., [Watkins, 2002]).

However, the potential problems with VBM-style approaches for data such as multisubject FA images have not yet been investigated fully. In particular, this use raises a serious question, which has not yet been satisfactorily answered: how can one guarantee that any given standard space voxel contains data from the same part of the same white matter (WM) tract from each and every subject? In other words, how can we guarantee that registration of every subject's data to a common space has been totally successful, both in terms of resolving topological variabilities and in terms of the exact alignment of the very fine structures present in such data? A second problem relates to the standard practice of spatially smoothing data before computing voxelwise statistics—the amount of smoothing can greatly affect the final results, but there is no principled way of deciding how much smoothing is the "correct" amount [Jones, 2005]. (Smoothing also increases effective partial voluming, a problem with VBM-style approaches particularly when applied to data such as FA; see Discussion for more comment on this.)

propose an approach to carrying out localised statistical testing of FA (and other diffusion-related) data that should alleviate the alignment problems. We project individual subjects' FA data into a common space in a way that is not dependent on perfect nonlinear registration. This is achieved through the use of (a) an initial approximate nonlinear registration, followed by (b) projection onto an alignment-invariant tract representation (the "mean FA skeleton"). No spatial smoothing is necessary in the image processing.

In essence, they have presented a new method for estimating localized change in fractional anisotropy, a useful marker for brain connectivity across different subjects. The method attempts to combine the strengths of voxel-based analyses (being able to analyse the whole brain without predefining voxels or tracts of interest) with the strengths of tractography-based analyses (ideally, being confident that the estimates of FA are truly taken from the relevant voxels). They have shown that by projecting FA values onto a subject-mean FA tract skeleton, cross-subject FA becomes more Gaussian and of lower variability; hence analyses become more robust and more sensitive.

## **Chapter 2. Structural Brain Imaging - An Introduction**

---

Obviously if two pre-specified the FA target image then this step is automatically skipped. The script then takes the target and affine-aligns it into 1x1x1mm MNI152 space - this resolution is chosen as the later skeletonisation and projection steps work well at this resolution, and the choice of working in MNI152 space is chosen for convenience of display and coordinate reporting later.

# 3 Tools Required

## 3.1 Principle Component Analysis - Dimensionality Reduction

Principal component analysis (PCA) [Jolliffe(2002)] is an old tool in multivariate data analysis. It was used already in 1901. The principal components are the eigenvectors of the covariance matrix. The projection of data onto the principal components is sometimes called the Hotelling transform after H. Hotelling or Karhunen-Lo`eve transform (KLT) after K. Karhunen and M. Lo`eve . This transformation is as an orthogonal transformation that diagonalizes the covariance matrix. It is obtained from the Singular Value Decomposition of the data matrix.

## 3.2 Canonical Correlation Analysis

Canonical correlation analysis (CCA) [Borga(2001)] is a way of measuring the linear relationship between two multidimensional variables. It finds two bases, one for each variable, that are optimal with respect to correlations and, at the same time, it finds the corresponding correlations. In other words, it finds the two bases in which the correlation matrix between the variables is diagonal and the correlations on the diagonal are maximized. The dimensionality of these new bases is equal to or less than the smallest dimensionality of the two variables. An important property of canonical correlations is that they are invariant with respect to affine transformations of the variables. This is the most important difference between CCA and ordinary correlation analysis which highly depend on the basis in which the variables are described. CCA was developed by H. Hotelling. Although being a standard tool in statistical analysis, where canonical correlation has been used for example in economics, medical studies, meteorology and even in classification of malt whisky, it is surprisingly unknown in the fields of learning and signal processing.

### 3.2.1 Definition

Canonical correlation analysis can be defined as the problem of finding two sets of basis vectors, one for  $x$  and the other for  $y$ , such that the correlations between the projections of the variables onto these basis vectors are mutually maximized. Let us look at the case where only one pair of basis vectors are sought, namely the ones corresponding to the largest canonical correlation: Consider the linear combinations  $x = x^T w_x$  and  $y = y^T w_y$  of the two variables respectively. This means that the function to be maximized is

$$\rho = \frac{E[xy]}{\sqrt{E[x^2]E[y^2]}} = \frac{w_x^T C_{xy} w_y}{\sqrt{w_x^T C_{xx} w_x w_y^T C_{yy} w_y}} \quad (3.1)$$

The maximum of  $\rho$  with respect to  $w_x$  and  $w_y$  is the maximum canonical correlation. The subsequent canonical correlations are uncorrelated for different solutions.

## 3.3 Hypothesis Testing

A hypothesis test is a statistical test that is used to determine whether there is enough evidence in a sample of data to infer that a certain condition is true for the entire population.

A hypothesis test examines two opposing hypotheses about a population: the null hypothesis and the alternative hypothesis. The null hypothesis,  $H_0$ , is the statement being tested. Usually the null hypothesis is a statement of "no effect" or "no difference". The alternative hypothesis,  $H_1$ , is the statement that we want to be able to conclude is true.

The value that is used to test the hypothesis is called the test statistic. It is defined as the standardized value that is calculated from sample data during a hypothesis test. The p-value, a measure that determines the statistical significance, is computed for the test statistic. Thereby, based on the sample data, the hypothesis test determines whether to reject the null hypothesis using the obtained p-value. If the p-value is less than or equal to the level of significance, which is a cut-off point that you define, then you can reject the null hypothesis.

### 3.3.1 Types of Errors

When hypothesis test is conducted, two types of errors are possible: Type I and Type II. The risks of these two errors are inversely related and determined by the level of significance and the power for the test. Therefore, one should determine which error has more severe consequences for the considered situation, before the risks are defined. No hypothesis test is 100% certain. Because the test is based on probabilities, there is always a chance of drawing an incorrect conclusion.

#### Type I Error

When the null hypothesis is true and is still rejected, a type I error is committed. The probability of making a type I error is  $\alpha$ , which is the level of significance set during the hypothesis test. An  $\alpha$  of 0.05 indicates that we are willing to accept a 5% chance that we are wrong when we reject the null hypothesis. To lower this risk, we must use a lower value for  $\alpha$ . However, using a lower value for alpha means that we will be less likely to detect a true difference if one really exists.

#### Type II Error

When the null hypothesis is false and is still not rejected, a type II error is said to be committed. The probability of making a type II error is  $\beta$ , which depends on the power of the test. The risk of committing a type II can be decreased by ensuring that the test has enough power. An alternate solution is by ensuring that the sample size is large enough to detect a practical difference when one truly exists.

#### 3.3.2 Hypothesis Tests and its test statistic

Data can either be continuous, discrete, binary, or categorical. Continuous, or interval, data have units that can be measured with a value anywhere between the lowest and the highest value. An example is platelet count. Discrete, or ordinal, data have a rank order, but the scale is not necessarily linear. A pain scale from 1 to 10 is a good example; a pain score of 8 is not necessarily twice as bad as 4. Binary data are simply yes/no data: alive or dead. Examples of categorical, or nominal, data are color or shape. The data are different, but no rank order exists. The test chosen to analyze the data is based on the type of data collected and some key properties of that data. Based on the type of data and the underlying population distribution, statistical hypothesis testing can be broadly classified into two categories:

1. Parametric Testing
2. Non-parametric Testing

#### Parametric Testing

Parametric tests are more robust and for the most part require less data to make a stronger conclusion than nonparametric tests. However, to use a parametric test, 3 parameters of the data must be true or are assumed. First, the data need to be normally distributed, which means all data points must follow a bell-shaped curve without any data skewed above or below the mean. For example, the Episodic memory scores for all subjects are normally distributed. Second, the data also need to have equal variance and have the same standard deviation. Finally, the data need to be continuous. Commonly used parametric tests are :

### **Chapter 3. Tools Required**

---

1. 1-sample t-test
2. 2-sample t-test
3. One-Way Analysis of Variance (ANOVA)

Some cases where parametric testing is useful are: (1) When the data distribution is skewed and non-normal; (2) When there are multiple groups with each having different spreads; (3) When higher statistical power is required where power is the measure of a test's ability to accurately detect that the null hypothesis is false

### **Non-Parametric Testing**

Non-parametric tests are sometimes called distribution-free tests because they are based on fewer assumptions (e.g., they do not assume that the outcome is approximately normally distributed). Parametric tests involve specific probability distributions (e.g., the normal distribution) and the tests involve estimation of the key parameters of that distribution (e.g., the mean or difference in means) from the sample data. The cost of fewer assumptions is that non-parametric tests are generally less powerful than their parametric counterparts (i.e., when the alternative is true, they may be less likely to reject  $H_0$ ). Commonly used non-parametric tests are:

1. 1-sample Sign, 1-sample Wilcoxon
2. Mann-Whitney test
3. Kruskal-Wallis, Mood's median test
4. Permutation Testing

There are some situations when it is clear that the outcome does not follow a normal distribution and non-parametric testing is the way to go. (1) When the outcome is an ordinal variable or a rank; (2) When there are definite outliers which cannot be removed; (3) When the outcome has clear limits of detection; (4) The sample size is very small.

They do have other assumptions that can be hard to meet. For non-parametric tests that compare groups, a common assumption is that the data for all groups must have the same spread (dispersion) if your groups have a different spread, the non-parametric tests might not provide valid results.

### **3.4 Permutation Testing**

Permutation tests [Efron and Tibshirani(1994)] are one type of nonparametric test. They were proposed in the early twentieth century, but have only recently become popular with the availability of inexpensive, powerful computers to perform the computations involved.

The essential concept of a permutation test is relatively intuitive. For example, consider a simple single subject PET activation experiment, where a single subject is scanned repeatedly under “rest” and “activation” conditions. Considering the data at a particular voxel, if there is really no difference between the two conditions, then we would be fairly surprised if most of the “activation” observations were larger than the “rest” observations, and would be inclined to conclude that there was evidence of some activation at that voxel. Permutation tests simply provide a formal mechanism for quantifying this “surprise” in terms of probability, thereby leading to significance tests and p-values.

If there is no experimental effect, then the labelling of observations by the corresponding experimental condition is arbitrary, because the same data would have arisen whatever the condition. These labels can be any relevant attribute: condition “tags,” such as “rest” or “active”; a covariate, such as task difficulty or response time; or a label, indicating group membership. Given the null hypothesis that the labellings are arbitrary, the significance of a statistic expressing the experimental effect can then be assessed by comparison with the distribution of values obtained when the labels are permuted.

The justification for exchanging the labels comes from either weak distributional assumptions, or by appeal to the randomization scheme used in designing the experiment. Tests justified by the initial randomization of conditions to experimental units (e.g., subjects or scans), are sometimes referred to as randomization tests, or re-randomization tests.

### **3.4.1 Permutation Test**

In many situations it is impractical to randomly allocate experimental conditions, or perhaps we are presented with data from an experiment that was not randomized. For instance, we can not randomly assign subjects to be patients or normal controls. Or, for example, consider a single subject PET design where a covariate is measured for each scan, and we seek brain regions whose activity appears to be related to the covariate value. In the absence of an explicit randomization of conditions to scans, we must make weak distributional assumptions to justify permuting the labels on the data. Typically, all that is required is that distributions have the same shape, or are symmetric. The actual permutations that are performed depend on the degree of exchangeability, which in turn depend on the actual assumptions made. With the randomization test, the experimenter designs the initial randomization scheme carefully to avoid confounds. The randomization scheme reflects an implicitly assumed degree of exchangeability. With the permutation test, the degree of exchangeability must be assumed post hoc. The reasoning that would have led to a particular randomization scheme can be usually be applied post-hoc to an experiment, leading to a permutation test with the same degree of exchangeability. Given exchangeability, computation proceeds as for the randomization test.

### 3.4.2 Considerations

#### Assumptions

Weak distributional assumptions are made, which embody the degree of exchangeability. The exact form of these assumptions depends on the experiment at hand, as illustrated in the following section and in the examples section. For a simple single subject activation experiment, we might typically assume the following. For a particular voxel, “active” and “baseline” scans within a given block have a distribution with the same shape, though possibly different means. The null hypothesis asserts that the distributions for the “baseline” and “active” scans have the same mean, and hence are the same. Then the labeling of scans is arbitrary within the chosen blocks, which are thus the exchangeability blocks. Any permutation of the labels within the exchangeability blocks leads to an equally likely statistic. The mechanics are then the same as with the randomization test. For each of the possible relabeling, compute the statistic of interest; for relabeling  $i$ , call this statistic  $t_i$ . Under the null hypothesis each of the  $t_i$  are equally likely, so the P-value is the proportion of the  $t_i$  greater than or equal to the statistic  $T$  corresponding to the correctly labeled data.

#### Number of relabelings and test size

A constraint on the permutation test is the number of possible relabelings. Because the observed labeling is always one of the  $N$  possible relabelings, the smallest P-value attainable is  $1/N$ . Thus, for a level  $\alpha = 0.05$  test to potentially reject the null hypothesis, there must be at least 20 possible labeling. More generally, the permutation distribution is discrete, consisting of a finite set of possibilities corresponding to the  $N$  possible relabelings. Hence, any P-values produced will be multiples of  $1/N$ . Further, the  $100(1 - \alpha)^{th}$  percentile of the permutation distribution, the critical threshold for a level  $\alpha$  test, may lie between two values. Equivalently,  $\alpha$  may not be a multiple of  $1/N$ , such that a P-value of exactly  $\alpha$  cannot be attained. In these cases, an exact test with size exactly  $\alpha$  is not possible. It is for this reason that the critical threshold is computed as the  $c + 1$  largest member of the permutation distribution, where  $c = \lfloor \alpha N \rfloor$ ,  $\alpha N$  rounded down. The test can be described as almost exact, because the size is at most  $1/N$  less than  $\alpha$ .

#### Power

Frequently, nonparametric approaches are less powerful than equivalent parametric approaches when the assumptions of the latter are true. The assumptions provide the parametric approach with additional information that the nonparametric approach must “discover.” The more labelings, the better the power of the nonparametric approach relative to the parametric approach. In a sense the method has more information from more labelings, and “discovers” the null distribution assumed in the parametric approach. If the assumptions required for a parametric analysis are not credible, however, a nonparametric approach provides the only

valid method of analysis.

## 3.5 Bootstrapping

In statistics, bootstrapping can refer to any test or metric that relies on random sampling with replacement. Bootstrapping allows assigning measures of accuracy (defined in terms of bias, variance, confidence intervals, prediction error or some other such measure) to sample estimates [Efron and Tibshirani(1994)]. This technique allows estimation of the sampling distribution of almost any statistic using random sampling methods. Generally, it falls in the broader class of resampling methods.

Bootstrapping is the practice of estimating properties of an estimator (such as its variance) by measuring those properties when sampling from an approximating distribution. One standard choice for an approximating distribution is the empirical distribution function of the observed data. In the case where a set of observations can be assumed to be from an independent and identically distributed population, this can be implemented by constructing a number of resamples with replacement, of the observed dataset.

### 3.5.1 Approach

The basic idea of bootstrapping is that inference about a population from sample data, (sample → population), can be modeled by resampling the sample data and performing inference about a sample from resampled data, (resampled → sample). As the population is unknown, the true error in a sample statistic against its population value is unknowable. In bootstrap-resamples, the 'population' is in fact the sample, and this is known; hence the quality of inference of the 'true' sample from resampled data, (resampled → sample), is measurable.

More formally, the bootstrap works by treating inference of the true probability distribution  $J$ , given the original data, as being analogous to inference of the empirical distribution of  $S$ , given the resampled data. The accuracy of inferences regarding  $J$  using the resampled data can be assessed because we know  $S$ . If  $S$  is a reasonable approximation to  $J$ , then the quality of inference on  $S$  can in turn be inferred.

### 3.5.2 Illustration

Assume we are interested in the average (or mean) height of people worldwide. We cannot measure all the people in the global population, so instead we sample only a tiny part of it, and measure that. Assume the sample is of size  $N$ ; that is, we measure the heights of  $N$  individuals. From that single sample, only one estimate of the mean can be obtained. In order to reason about the population, we need some sense of the variability of the mean that we have computed. The simplest bootstrap method involves taking the original data set of  $N$  heights, and, using a computer, sampling from it to form a new sample (called a 'resample' or

## **Chapter 3. Tools Required**

---

bootstrap sample) that is also of size N. The bootstrap sample is taken from the original by using sampling with replacement so, assuming N is sufficiently large, for all practical purposes there is virtually zero probability that it will be identical to the original "real" sample. Since we are sampling with replacement, we are likely to get one element repeated, and thus every unique element be used for each resampling. This process is repeated a large number of times (typically 1,000 or 10,000 times), and for each of these bootstrap samples we compute its mean (each of these are called bootstrap estimates). We now have a histogram of bootstrap means. This provides an estimate of the shape of the distribution of the mean from which we can answer questions about how much the mean varies. (The method here, described for the mean, can be applied to almost any other statistic or estimator.)

### **3.5.3 Discussion**

#### **Advantages**

A great advantage of bootstrap is its simplicity. It is a straightforward way to derive estimates of standard errors and confidence intervals for complex estimators of complex parameters of the distribution, such as percentile points, proportions, odds ratio, and correlation coefficients. Bootstrap is also an appropriate way to control and check the stability of the results. Although for most problems it is impossible to know the true confidence interval, bootstrap is asymptotically more accurate than the standard intervals obtained using sample variance and assumptions of normality.

#### **Dis-advantages**

Although bootstrapping is (under some conditions) asymptotically consistent, it does not provide general finite-sample guarantees. The apparent simplicity may conceal the fact that important assumptions are being made when undertaking the bootstrap analysis (e.g. independence of samples) where these would be more formally stated in other approaches

#### **Recommendations**

The number of bootstrap samples recommended in literature has increased as available computing power has increased. If the results may have substantial real-world consequences, then one should use as many samples as is reasonable, given available computing power and time. Increasing the number of samples cannot increase the amount of information in the original data; it can only reduce the effects of random sampling errors which can arise from a bootstrap procedure itself.

## 3.6 Procrustes Analysis

In statistics, Procrustes analysis is a form of statistical shape analysis used to analyse the distribution of a set of shapes.

To compare the shapes of two or more objects, the objects must be first optimally "superimposed". Procrustes superimposition (PS) is performed by optimally translating, rotating and uniformly scaling the objects. In other words, both the placement in space and the size of the objects are freely adjusted. The aim is to obtain a similar placement and size, by minimizing a measure of shape difference called the Procrustes distance between the objects. This is sometimes called full, as opposed to partial PS, in which scaling is not performed (i.e. the size of the objects is preserved). Notice that, after full PS, the objects will exactly coincide if their shape is identical. For instance, with full PS two spheres with different radii will always coincide, because they have exactly the same shape. Conversely, with partial PS they will never coincide. This implies that, by the strict definition of the term shape in geometry, shape analysis should be performed using full PS. A statistical analysis based on partial PS is not a pure shape analysis as it is not only sensitive to shape differences, but also to size differences. Both full and partial PS will never manage to perfectly match two objects with different shape, such as a cube and a sphere, or a right hand and a left hand.

In some cases, both full and partial PS may also include reflection. Reflection allows, for instance, a successful (possibly perfect) superimposition of a right hand to a left hand. Thus, partial PS with reflection enabled preserves size but allows translation, rotation and reflection, while full PS with reflection enabled allows translation, rotation, scaling and reflection.

In mathematics:

- (i) an orthogonal Procrustes problem is a method which can be used to find out the optimal rotation and/or reflection (i.e., the optimal orthogonal linear transformation) for the PS of an object with respect to another.
- (ii) a constrained orthogonal Procrustes problem, subject to  $\det(R) = 1$  (where R is a rotation matrix), is a method which can be used to determine the optimal rotation for the PS of an object with respect to another (reflection is not allowed). In some contexts, this method is called the Kabsch algorithm.

### 3.6.1 Algorithm

There are two ways to perform procrustes analysis:

#### Analytic Method

Consider objects made up from a finite number  $k$  points in  $n$  dimensions. Often, these points are selected on the continuous surface of complex objects, such as a human bone, and in this case they are called landmark points.

### Chapter 3. Tools Required

---

The shape of an object can be considered as a member of an equivalence class formed by removing the translational, rotational and uniform scaling components.

The alignment part involves four steps:

1. Compute the centroid of each shape.
2. Re-scale each shape to have equal size.
3. Align w.r.t. position the two shapes at their centroids.
4. Align w.r.t. orientation by rotation

On alignment the Singular Value Decomposition (SVD) is applied:

1. Arrange the size and position aligned  $x_1$  and  $x_2$  as  $n \times k$  matrices (in the planar case  $k = 2$ ).
2. Calculate the SVD,  $UDV^T$ , of  $x_1^T x_2$  in order to maximize the correlation between the two sets of landmarks.
3. The rotation matrix needed to optimally superimpose  $x_1$  upon  $x_2$  is then  $VU^T$ .

$$\begin{bmatrix} \sin(\theta) & -\sin(\theta) \\ \sin(\theta) & \cos(\theta) \end{bmatrix} \quad (3.2)$$

### Generalized Procrustes Analysis

All though an analytic solution exists [12, 7] to the alignment of a set of planar shapes the following iterative approach to generalized Procrustes analysis [1, 5] will suffice. •

1. Choose an initial estimate of the mean shape (e.g. the first shape in the set).
2. Align all the remaining shapes to the mean shape.
3. Re-calculate the estimate of the mean from the aligned shapes.
4. If the estimated mean has changed return to step 2.

Convergence is thus declared when the mean shape does not change significantly within an iteration.

### 3.7 Brain Atlas

A brain atlas is composed of serial sections along different anatomical planes of the healthy or diseased developing or adult animal or human brain where each relevant brain structure is assigned a number of coordinates to define its outline or volume. Brain atlases are contiguous, comprehensive results of visual brain mapping and may include anatomical, genetical or functional features. One of the most widely-used atlases is one by Talairach and Tournoux [Talairach and Tournoux(1988)], which is based on histology data from a single subject. The atlas contains a cytoarchitectural map of the cortex through the addition of Brodmann's map [Brodmann(1909)], explaining its wide use for registering, identifying, and reporting human cortical locations in a common coordinate system [Lancaster(2000)]. A series of probabilistic maps provided by the Montreal Neurological Institute (MNI) and the International Consortium of Brain Mapping (ICBM) are also widely used [Collins(1994); Evans(1992); Mazziotta(1995)]. These maps were created by linearly registering a large number of T1-weighted MR images of normal subjects into a common template. These maps have excellent values as a target template for normalization-based group analyses. However, in these existing atlases, the amount of information about white matter anatomy is limited [Toga(2006)]. This lack of white matter information is understandable because this tissue appears homogeneous in conventional MRI, as well as in histology preparations. Such a lack of anatomical clues, contrary to gyral and sulcal patterns in the cortex, renders identification and delineation of specific white matter locations very difficult.

Diffusion tensor imaging is a relatively new MR modality, with which we can visualize various axonal bundles within the white matter, based on orientational information. This orientation-based contrast opens up new opportunities to establish a white matter coordinate system and study disease mechanisms or relationship between anatomy and functions of white matter. To understand disease patterns (e.g., the lesion frequency in a specific white matter location) or to correlate these anatomic abnormalities with functional deficits using group statistical analyses, lesion locations must be described by a coordinate system. DTI information can be used to generate "addresses" based on anatomic units in otherwise homogeneous-looking white matter, which is the first step toward the establishment of a white matter functional map similar to cortical functional maps. Establishing a standard coordinate system for white matter and developing tools to utilize it are thus of great importance. In this paper, we introduce a stereotaxic population[SM1]-averaged white matter atlas, in which we fused DTI-based white matter information with an existing anatomical template (ICBM-152) [Oishi et al.(2009)]. This atlas is based on tensor maps obtained from 81 normal subjects acquired under an initiative of the International Consortium of Brain Mapping (ICBM). A hand-segmented white matter parcellation map [Oishi et al.(2009)] was created from this averaged map, which can be used for automated white matter parcellation. The precision of the affine-based image normalization and automated parcellation was measured for a group of normal subjects using manually defined anatomical landmarks. The axial slices of the atlas has been shown in Fig. 3.1.

## **Chapter 3. Tools Required**

---

In the WMPM, the following white matter structures are identified and partitioned:

### **Tracts in the brainstem**

**Corticospinal tracts (CST):** This structure can be clearly identified at the medulla and the pons level, but should also contain corticopontine and corticobulbar tracts.

**Medial lemniscus (ML):** This is a major sensory pathway toward the thalamus. This tract is identifiable in the pons, but not in the midbrain. Because of the limited image resolution, this parcellation may include the central tegmental tract.

**Medial longitudinal fasciculus (MLF):** This fiber bundle, running along the medial dorsal aspect of the brainstem, connects various nuclei in the brainstem.

**Inferior cerebellar peduncle (ICP):** This tract carries information from the spinal cord and the medulla to the cerebellum.

**Middle cerebellar peduncle (MCP):** This massive tract initiates from the pontine nuclei and carries information between the cortex and the cerebellum.

**Superior cerebellar peduncle (SCP):** This tract carries information between the deep cerebellar nuclei (dentate nuclei) and the thalamus. This tract is identifiable from the cerebellar nuclei to the midbrain at the SCP decussation. After the decussation, the tract cannot be identified with current image resolution.

### **Projection fibers**

**Corona radiata:** This structure is divided into three regions: anterior (ACR), superior (SCR), and posterior (PCR). The divisions are made at the middle of the genu and splenium of the corpus callosum, which are arbitrarily chosen and not based on anatomic or functional boundaries.

**Anterior limb of internal capsule (ALIC):** The anterior thalamic radiation and fronto-pontine fibers are the major contributors in this region.

**Posterior limb of internal capsule (PLIC):** The superior thalamic radiation and long corticofugal pathways, such as the corticospinal tract and the fronto- and parieto-pontine fibers, are the major constituents.

**Retrolenticular part of the internal capsule (RLIC):** In this region, the posterior thalamic radiation (cortico-thalamic and thalamo-cortical fibers, including the optic radiation) is the major constituent, but can also include the parieto-, occipito- and temporo-pontine fibers. The boundary with the sagittal stratum (SS) is arbitrarily defined at the middle of the splenium of the corpus callosum.

**Cerebral peduncle (CP):** This is a region where long corticofugal pathways are concentrated, including the corticospinal, corticopontine, and corticobulbar tracts. The [SM15] boundary between the cerebral peduncle and the internal capsule is defined at the axial level below the anterior commissure.

### Association fibers

**Superior longitudinal fasciculus (SLF):** This tract locates at the dorsolateral regions of the corona radiata and contain connections between the frontal, parietal, occipital, and temporal lobes including language-related areas (Broca's, Geschwind's, and Wernicke's territories).

**Superior fronto-occipital fasciculus (SFO):** This tract is located at the superior edge of the anterior limb of the internal capsule (anterior thalamic radiation) and the boundary is not always clear.

**Uncinate fasciculus (UNC):** This tract connects the frontal lobe (orbital cortex) and the anterior temporal lobe. It can be discretely identified where the two lobes are connected but not within the frontal and the temporal lobes where it merges with other tracts.

**Inferior fronto-occipital fasciculus (IFO) / Uncinate fasciculus (UNC):** The IFO connects the frontal lobe and the occipital lobe. In the frontal lobe, this partition also includes the frontal projection of the UNC. In the temporal and occipital lobe, the IFO merges with the inferior longitudinal fasciculus (ILF), which is segmented as a different partition.

**Inferior fronto-occipital fasciculus (IFO) / inferior longitudinal fasciculus (ILF):** This partition includes the white matter in the temporal and occipital lobe where the IFO and the ILF are the major constituents. The ILF connects the temporal lobe and the occipital lobes. It cannot be distinguished from the IFO in most of the temporal and occipital white matter.

**Sagittal Stratum (SS):** The IFO/ILF merges with projection fibers from the RLIC and forms a large, sheet-like, sagittal structure, called the sagittal stratum. This region, therefore, should include both association and projection fibers. The boundary of the IFO/ILF and SS is arbitrarily defined at the axial level of the anterior commissure.

**External capsule (EC):** This region, located lateral to the internal capsule, is believed to contain association fibers, such as the SLF and IFO and commissural fibers. Because of the limited image resolution, the external and extreme capsules are not resolved. **Cingulum (CG):** This tract carries information from the cingulate gyrus to the hippocampus. The entire pathway from the frontal lobe to the temporal lobe can be clearly identified. In the WMPM, the CG in the cingulate gyrus and the hippocampal regions is separated at the axial level of the splenium of the corpus callosum and denoted as CgC and CgH, respectively.

**Fornix (FX) and stria terminalis (ST):** These tracts are both related to the limbic system: the FX to the hippocampus, and the ST to the amygdala. Both tracts project to the septum and the hypothalamus.

### Commissural fibers

**Anterior commissure (AC):** The projection to the temporal lobes of the AC is segmented.

**Corpus callosum (CC):** This partition contains the corpus callosum and the boundary extends until it merges with the corona radiata. The [SM16] CC is further divided into the genu (GCC), the body (BCC), and the splenium (SCC) regions with arbitrary boundaries.

**Tapetum (TAP):** This temporal component of the CC is partitioned separately from the other

## **Chapter 3. Tools Required**

---

CC regions. The current WMPM does not include the partition of subcortical white matter because of difficulties in assigning and defining boundaries in these regions.

### **3.7.1 Using the Atlas**

From a procedural point of view, there are two ways to use atlases. One is to warp the atlas to individual data and the other is to warp the individual data to the atlas. By applying the WMPM in the native space, we can automatically parcellate the WM without image interpolation, and it is more straightforward to perform volume measurements of each parcellated compartment. If one is interested in TBSS, images need to be warped to the atlas space. In this approach, the anatomical information, such as regional volume changes, is stored in the transformation matrix and can be retrieved by using metrics such as Jacobian determinant. After VBA or TBSS analysis, the WMPM can be superimposed to evaluate which WM regions are affected. In addition to this type of qualitative utility, quantitative values can also be extracted by applying the WMPM and averaging the values of all pixels within one compartment (atlas-based analysis or ABA). For the VBA, statistics for each pixel are derived individually. This often leads to low statistical power necessitating the frequent use of spatial filtering for pixel averaging. The filter is usually isotropic. However, some reports have criticized the use of such a filtering procedure, especially for the WM structures, because of sharp transitions in structural units; tracts with very different functions could be only a few pixels away. The ABA could be considered a special kind of filtering that groups pixels belonging to a specific WM unit. This, however, assumes that abnormality follows WM anatomical boundaries. Depending on pathology, this is not always the case (e.g., vasculature-dependent diseases). Therefore, VBA and ABA should be considered complementary methods.

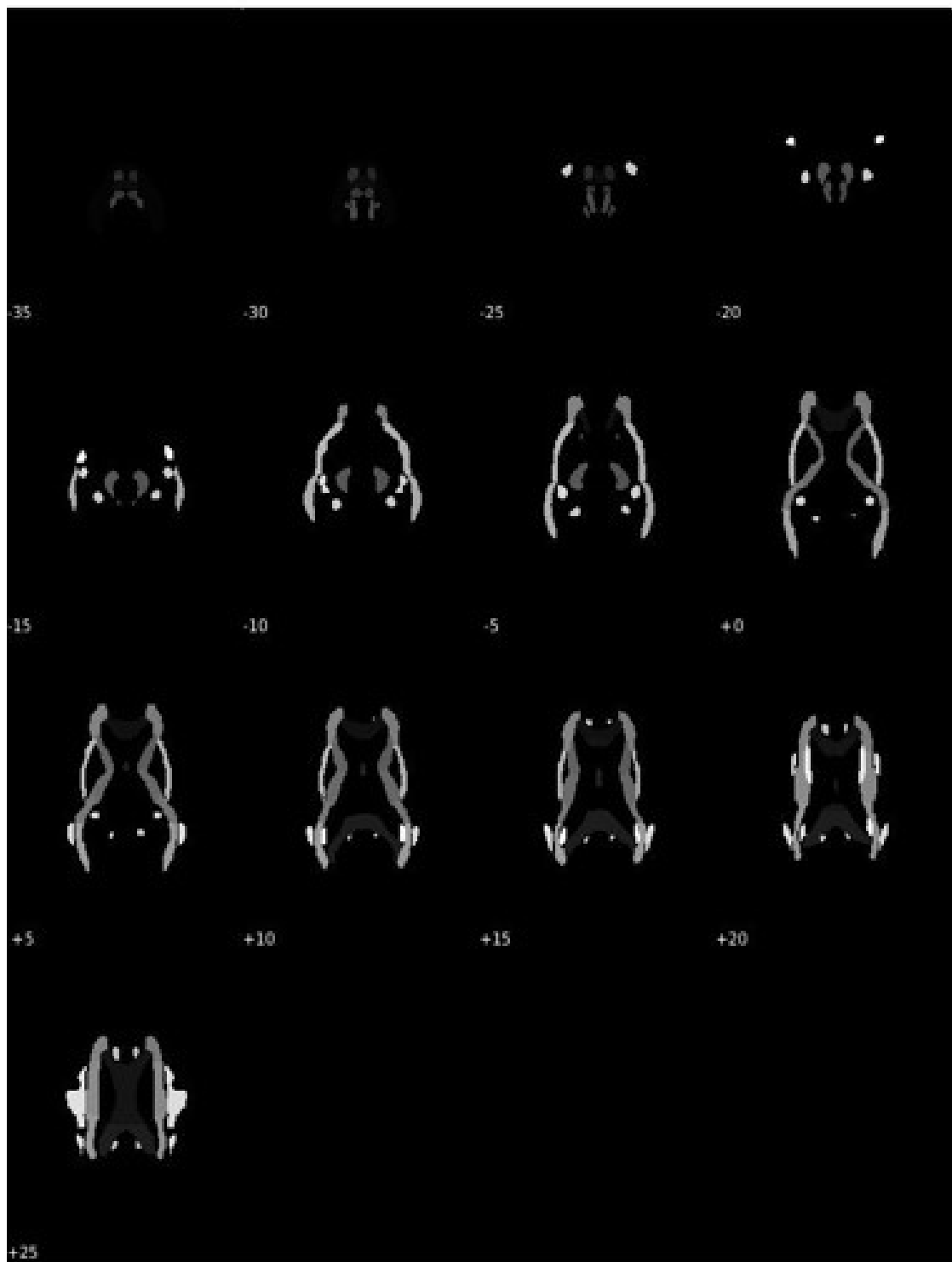


Figure 3.1 – Axial Slices of the Atlas



# 4 Methodology

In this chapter, the general pipeline used for analysis of imaging modality and behavioral measures has been explained in detail.

## 4.1 Data Preparation and Analysis:

### 4.1.1 Categorization of Data

There are three kinds of subjects (out of 377) involved in the analysis-

- Stable Controls (sCON) – 163 subjects (Normal unaffected subjects)
- Deteriorated Controls (dCON) – 157 subjects (Showing signs of AZD)
- Mild Cognitive Impairment (MCI) – 57 patients (Dementia State )

### 4.1.2 Imaging Data:

The preprocessed brain imaging data of each subject was subjected to masking to extract only the desired portion from the 4-Dimensional voxel space. The imaging data was prepared for analysis by placing each subject's masked voxel intensity information row-wise followed by standardized to have zero-mean and unit variance, across voxels of the subjects. This step is critical as dimensionality reduction step is affected by relative scaling of each variable.

This standardized data matrix was dimensionality reduced by Singular Value Decomposition (*SVD*), and the desired number of principle components were chosen based on two methodologies firstly, using the traditional method of considering the percentage of total variance preserved (atleast 70 percent) and secondly, according to Machinko Pastur's criteria for high-dimensional data. It is critical to find the optimum number of principle components as choosing large number of components leads to overfitting and more importantly, the later components just learn noise instead of meaningful information.

## **Chapter 4. Methodology**

---

The brain maps of some principle components has been shown in the figure below. It was observed that the region represented by each principle component considered is smooth carrying structural information without arbitrary noise-like structure characteristic of a undesirable principle component.

### **4.1.3 Behavioral Measures:**

The subject behavioral measures comprises of demographic measures namely, age and gender, neuropsychological measures - Mini-Mental State Examination (MMSE) and Verbal Episodic Memory (VEM)and NEO-Personal Inventory measures. Each subject measures were subjected to a rank-based inverse Gaussian transformation, to enforce Gaussianity for each of the SMs. This transformation was used to avoid undue influence of potential outlier values. Thereby, in this way both the imaging and behavioral data matrices were prepared for statistical analysis.

## **4.2 Statistical Testing:**

Then on preparing the two datasets, they are subjected to cononical correlation analysis as shown in Fig. ???. The correlation values are obtained and are then our hypothesis was tested for statistical significance. During which we use correlation as our test statistic as it takes on different values under the null hypothesis and other alternatives. Then, the sampling distribution of the test statistic is constructed when the null hypothesis is true and the p-value for the hypothesis, giving the probability that the test statistic would be at least as extreme as we observed, is computed. Permutation test was used to compute the sampling distribution by randomly shuffling the correlations and thus, make up as many data sets as we like. If the null hypothesis is true the shuffled data sets should look like the real data, otherwise they should look different from the real data. The ranking of the real test statistic among the shuffled test statistics gives a p-value. Hence, the significance of the mode obtained from CCA was tested using permutation testing with 10000 permutations and  $\alpha = 0.05$ .

## **4.3 Imaging and Behavioral Saliency Vector**

If there exists a significant mode of correlation with p-value less than 0.05 then the consistency of the results derived from this significant mode was tested by bootstrapping over folds of data. Bootstrapping is the general procedure of reapplying the same pipeline to random subsets of the data, but this with the presumed relation intact (i.e., that is were it differs from permutation testing). Each time random subset is taken and is passed through the pipeline, that's called a fold.

In our case, realigning the linear spaces across folds is also performed using Procrustes (i.e., this is a common procedure in for instance partial least squares techniques). Then, average across folds a significant mode (i.e., its weights for both modalities in case of CCA). Which has

### 4.3. Imaging and Behavioral Saliency Vector

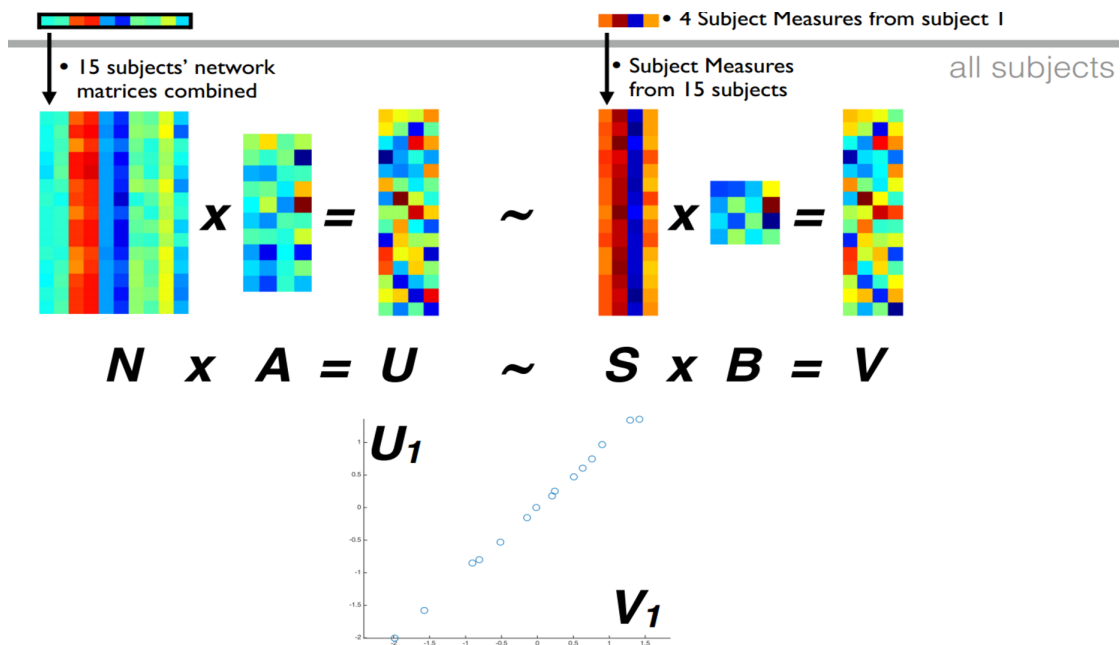


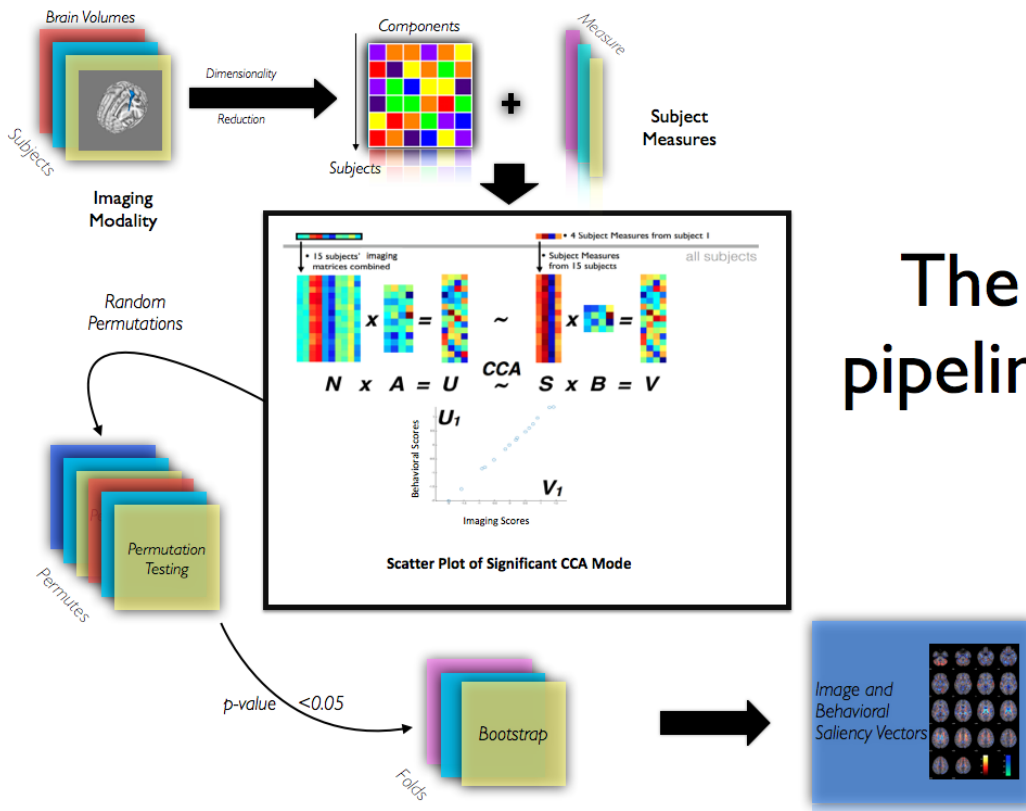
Figure 4.1 – Visualization of Canonical Correlation Analysis

been used to generate a brain map based on the bootstrap average, and bootstrap standard deviation constructed using simple combinations of variances (i.e., pooled variance). In this way, we establish the brainmap in terms of bootstrap ratio, which is interpretable as a z-score that indicates the consistency of the result across bootstrap folds.

On thresholding the brain maps based on the derived bootstrap ratio, the image saliency vector is derived, highlighting the regions of the brain which have shown constant and consistent relationship with its corresponding behavioral metrics. Bootstrapping can be performed either in the principle component space, where weights given to each component to obtain the maximally correlated mode are bootstrapped, or in the 4-dimensional voxel space, where the CCA mode weights of each fold is further used to return back to the brain voxel space and here, bootstrapping is performed.

Behavioral Saliency Vector was also constructed by performing bootstrapping over folds but now with CCA mode weights assigned to behavioral measures. It is necessary to correct the sign of the CCA modes while averaging over folds by initially choosing a reference mode, following which the modes are averaged across folds by flipping the sign of both imaging and behavior weights, if the mode obtained has negative correlation with the reference mode. Thus, averaging over folds is now safe to perform and the resulting saliency vector can be considered for drawing clinical conclusions.

The aforementioned pipeline has been summarized in Fig. 4.2 which gives a clear picture about each stage of the pre-processing.



## The pipeline

Figure 4.2 – The Pipeline

# 5 Results and Discussion

In this chapter, the results obtained for the three imaging modality investigated namely, Cerebral Blood Flow (CBF), Arterial Spin Labelling (ASL) based perfusion imaging and Tract Based Spatial Statistic (TBSS) has been explained.

## 5.1 Arterial Spin Labelled Imaging

ASL signal-to-noise ratio (SNR) is inherently low, because the signal from the labeled inflowing blood is only 0.5%-1.5% of the full tissue signal. The temporal resolution is also inherently poor. The low SNR combined with the poor temporal resolution results in a low contrast-to-noise ratio (CNR).

Further, since ASL is a subtraction technique, it is also sensitive to subject movement. Filters have been developed to detect and discard bad subtraction pairs related to large movements or transient hardware gradient malfunctions. However, the best way to ensure a proper subtraction of labeled from control scans is to use fast imaging techniques, such as spiral or EPI which has comes with the problem of low signal to noise ratio.

Though good parametric test results were obtained on performing CCA with Correlation of the significant mode being >90 percent and parametric p-value of  $< 0.05$  (0.0173). On performing permutation, it turned out to be dud with p-value of 0.279.

As a sanity test, steps were repeated by :

- Increasing the principle components to (75, 100).
- Incorporating all the subjects (sCON, dCON at MCI)

But still did not yield statistical significant results. Given the noisiness of the data and the lack of morphological distinctions seen in terms of the intensity values (read, features) as seen in Fig. 5.1 the result obtained was not a surprise.

## **Chapter 5. Results and Discussion**

---

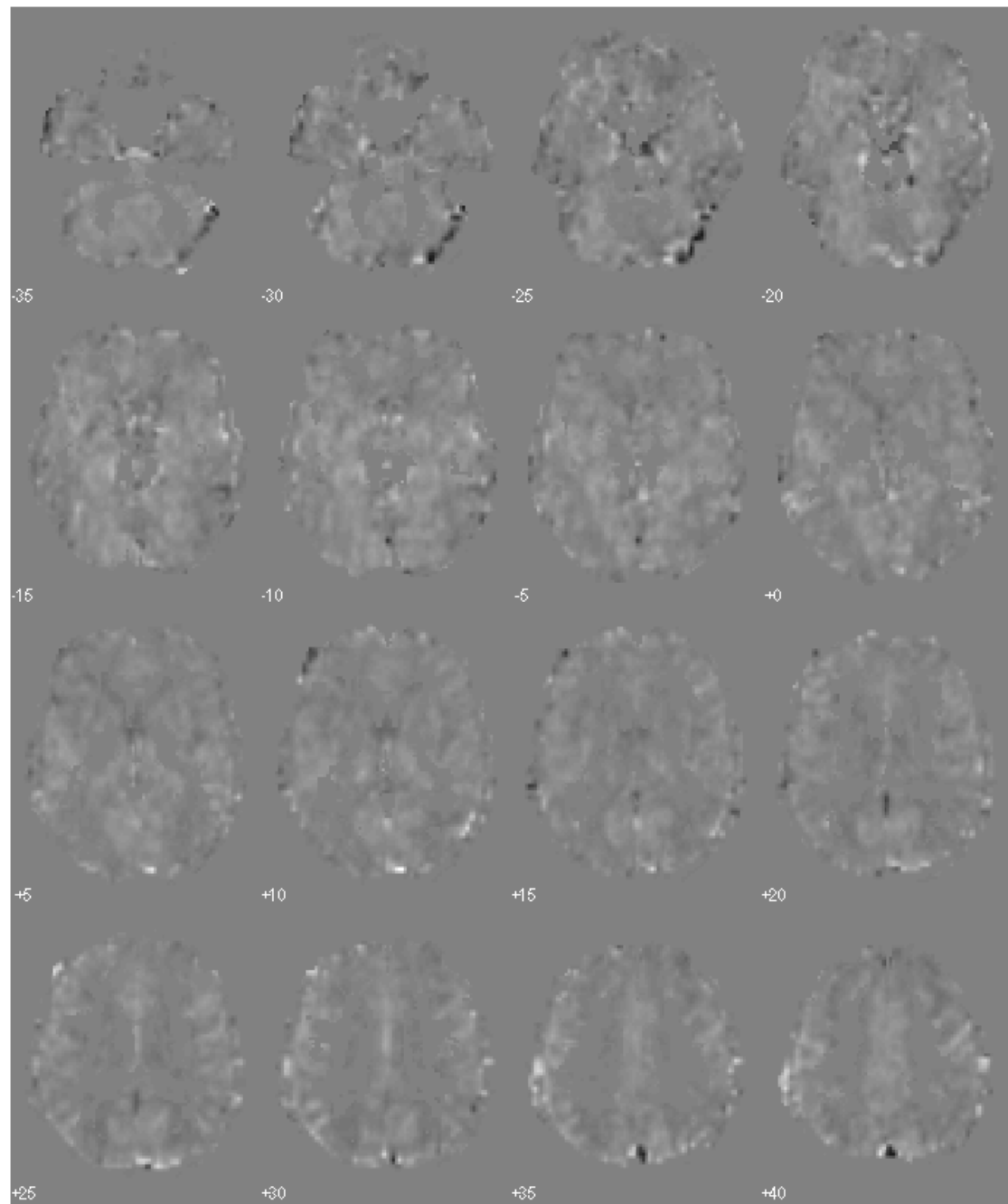


Figure 5.1 – An Example ASL image of a deteriorated control subjects.

## 5.2 3D T1 with Accentuated Grey Matter

This modality gave statistically significant result when 37 and 50 components were preserved. The results for the same are as follows:

- (a) 37 Principle Components:
  - 1. Correlation : 0.883
  - 2. Wilks test\*: 2.244e-06
  - 3. p-value\* : 0.034
  - 4. p-value (permutation test): 0.037
  
- (b) 50 Principle components:
  - 1. Correlation: 0.8985
  - 2. Wilks test\*: 1.21e-08
  - 3. p-value \*: 0.48
  - 4. p-value (permutation test): 0.091

However, it was not considered because: (a) Brain maps of components were not smooth and mostly, learning noise; (b) On PCA 1st component captures just 3% of total variance and the rest in the orders of 0.5-1.5%. This implies that the component was just learning noise and not any useful information. The Brain Saliency Vector shown in Fig. 5.2 proves that the maps does not make such sense anatomically and was hence, not pursued for future analysis.

## 5.3 Fractional Anisotropy

Each of the subjects data was masked using the FMRIB brain mask available on FSL before passing the data through the pipeline. The number of components preserved was 10 and 150 based on Marchenko Pastur's heuristic and the criterion to preserve atleast 70 percentage of total Variance which yielded correlation of 35.7 % and 80.3 % respectively. Following which the data were passed through the pipeline to test for statistical significance by permutation testing and consistency via bootstrapping. It was later observed that the p-value obtained by permutation testing was statistically significant for a single mode with p-value of 0.020 and 0.019 respectively. Then, bootstrapping was performed to derive the bootstrap ratio for the construction of imaging and behavioral saliency vector. The brain saliency vector for both the cases has been shown in Fig. 5.3 and the corresponding behavioural saliency vector is shown in Fig. 5.3. From Fig. 5.3, it can be observed that brain saliency vector derived using only 10 components make more sense in comparison to the one derived using 150 components - proving the use of Marchenko Pastur heuristic. It can also be observed in Fig. 5.3 that postive traits are obtaining positive weights and negative traits like Neuroticism and MMSE are getting negative traits proving the fidelity of the analysis.

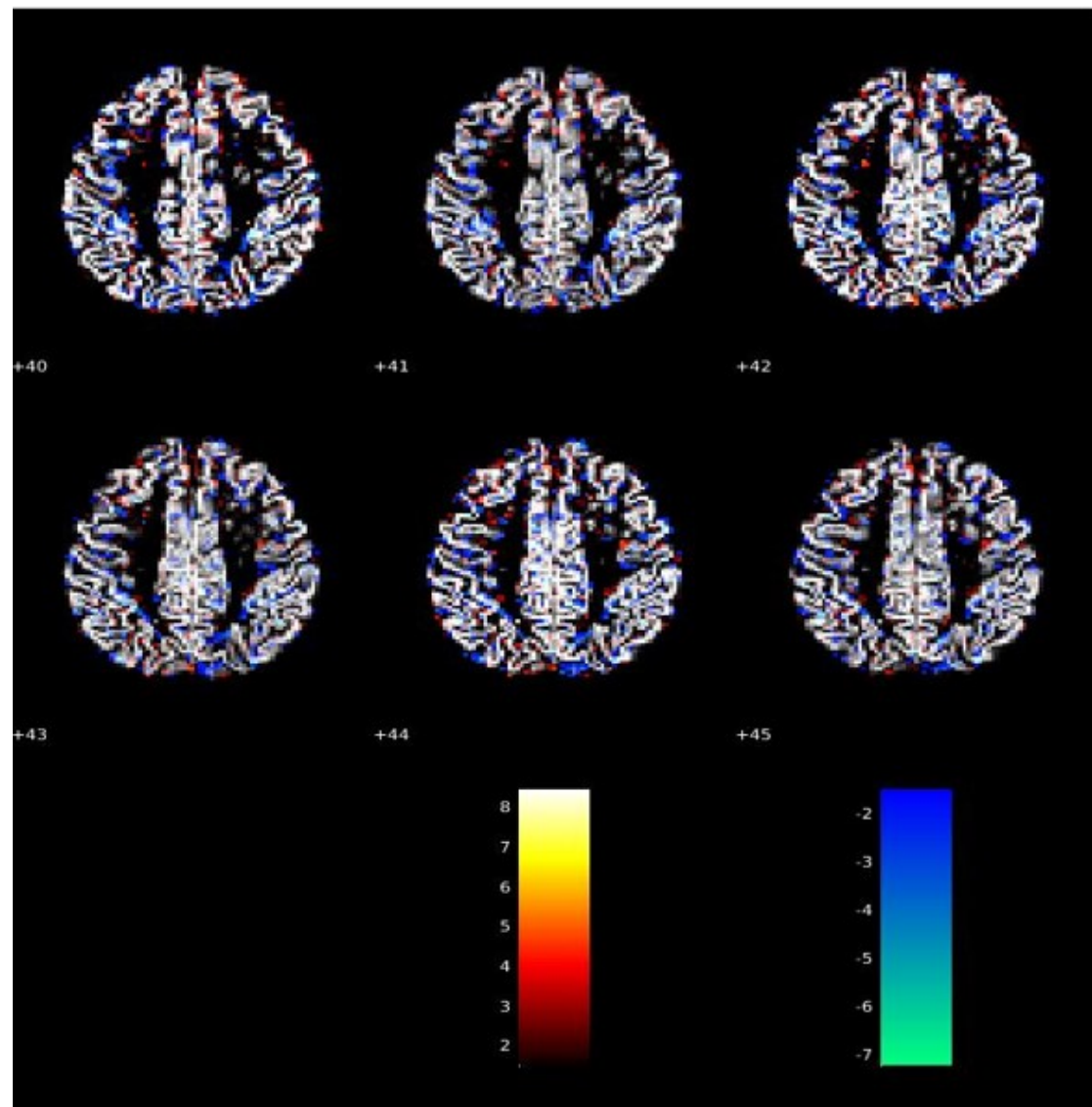


Figure 5.2 – Brain Saliency Vector when 37 Principle Components were preserved with Red showing positive correlation and blue representing negative Correlation

However, when the maps were shown to our radiologist for clinical tests, we realized that FA Maps were too diffuse and the image registration algorithms for FA are not optimal for voxel-based analysis. Thus, the results obtained were irrelevant for clinical use.

## **5.4 Tract Based Spatial Statistics**

In order to address the problem faced by diffusion data while conducting voxel-by-voxel analysis, a method called Tract-Based Spatial Statistics was introduced. This method is known for its carefully tuned image registration and projection onto an alignment invariant tract representation – Mean FA Skeleton which makes it robust for voxel based analysis.

### **5.4.1 Pre-processing of Fractional Anisotropy Data**

The steps involved in extraction of TBSS from FA data is summarized as follows.

#### **Step 1: Creation of FA data from a diffusion MRI study (A Protocol)**

- On correcting the data for head movement and eddy current, a brain mask is developed using one of the B=0 (no diffusion weighting) images. Following which diffusion tensor model is derived.

#### **Step2: Non-Linear Registration and Affine Transformation**

- On aligning all the FA images to 1 X 1 X 1 mm standard space. The target image used in the registrations can be A predefined target is automatically / manually chosen to be the most "typical" subject in the study. This is what I rephrased as arbitrary. There exists a FMRIB58-FA standard subspace image (used later to develop the custom mask) which can be used as the target in the TBSS.
- On using this , a single registration is performed per subject and generally, gives good alignment results. Third and the most cumbersome of all is to align each FA image with every other one and identify the "most representative" image which could be used as a target image. The method used to recognize the "most representative" image is explained in Step  
NOTE: We have used method 3 while pre-processing the images.
- The target image is then affine-aligned into MNI152 standard space, and every image is transformed into 1X1X1mm MNI 152 space by combining the non-linear transform to the target FA image with the affine transform from that target to MNI-152 space.

#### **Step 3: Back to the Standard Space**

- In this step, the non-linear transforms found in the previous stage to all subjects to bring them back into standard space. (If the third method of choosing target image was used then

## Chapter 5. Results and Discussion

---

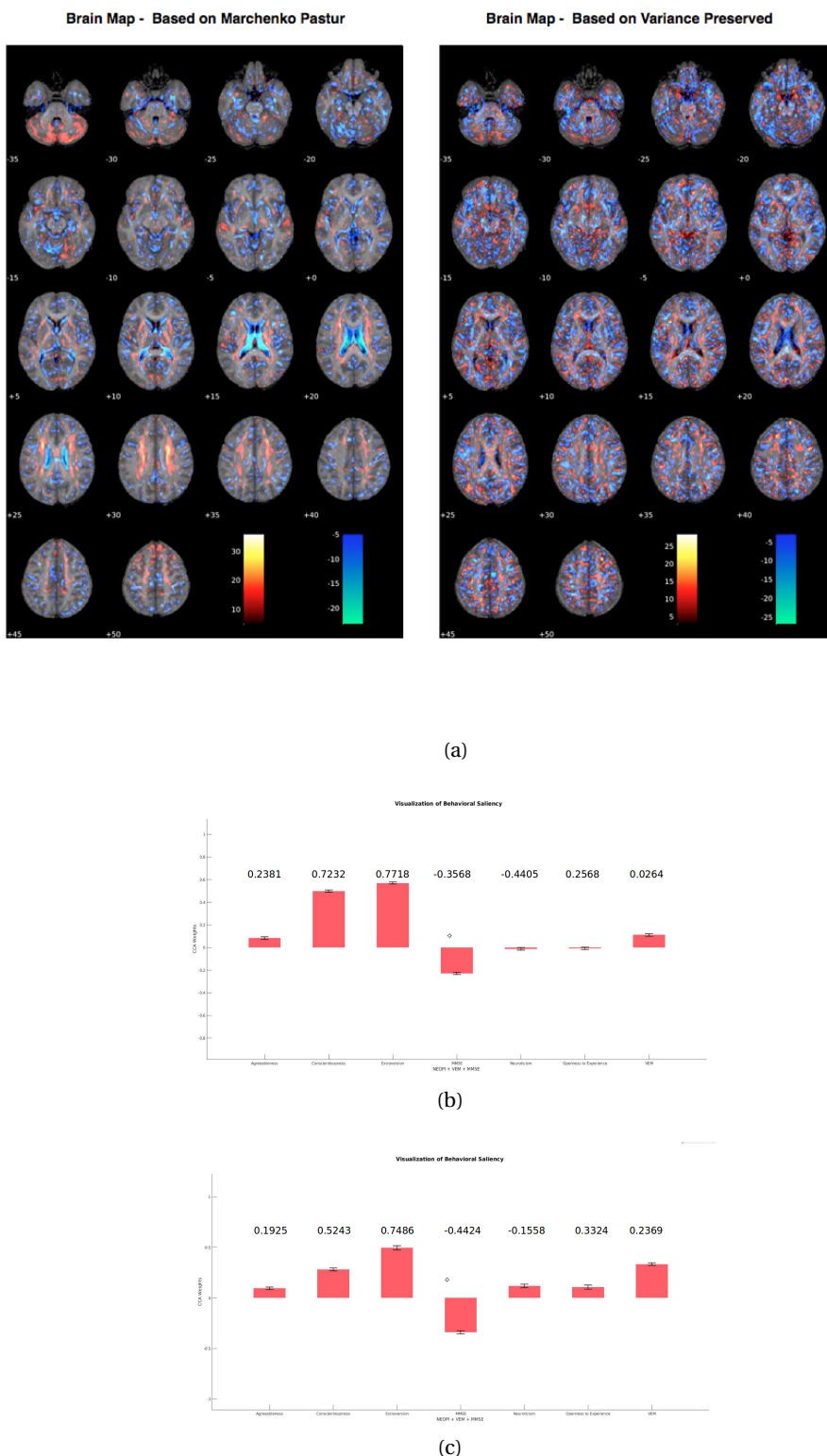


Figure 5.3 – Brain Saliency Vector when 10 and 100 Principle Components were preserved with Red showing positive correlation and blue representing negative Correlation; (b) Behavioral Saliency Vector and Behavioral Saliency Vector (c)

## **5.5. Results using TBSS - A Combination of Behaviors Approach**

---

the "most representative" image is chosen by estimating the average amount of warping that was necessary to align all other images to it, then uses the one which had the smallest amount of average warping when used as target.)

- In essence, the target is taken and affine-aligned into 1x1x1mm MNI152 space - this resolution was chosen as the later skeletonisation and projection steps work well at this resolution, and the choice of working in MNI152 space was chosen for convenience of display and coordinate reporting later.
- Thus , at the end of this stage, each subject's FA image has been nonlinear transformed to the target and then the affine transform to MNI152 space applied, resulting in a transformation of the original FA image into MNI152 space. The FSL toolbox combines the two transformations before being applying, to avoid having to resample the image twice

### **Step 4: FA Skeletonisation**

- Using, the subjects FA images in the standard space, mean FA image is obtained. Though the FMRI58-FA mean FA image and its derived skeleton could be used, the former is used as it is derived from the subjects used in the study.
- The threshold for the mean FA Skeleton is obtained (generally, 0.2 is good). This step is performed to suppress areas of low mean FA and/ or high inter-subject variability.
- Following which, we project each subject's (aligned) FA image onto the skeleton, by filling the skeleton with FA values from the nearest relevant tract centre. This is achieved, for each skeleton voxel, by searching perpendicular to the local skeleton structure for the maximum value in the subject's FA image. Thus, the following images obtained are ready for analysis.

## **5.5 Results using TBSS - A Combination of Behaviors Approach**

The analysis is divided into two subsections namely:

- Stable Controls
- Stable and Deteriorated Controls

### **5.5.1 Stable Controls**

#### **Principle Components Preservation**

In Figure 5.4 (a) you can observe the cumulative increase percentage variance preserved with number of principle components. It is based on this curve that we initially decided to chose the number of components to be preserved. However, as it was shown earlier that too many components were leading to formation of brain maps with blobs which are could not be interpreted, we choose the components based on Marchenko's pastur whose plot is shown in

## Chapter 5. Results and Discussion

---

Table 5.1 – P-value and Correlation Plot for Marchenko Pastur

R	0.49
p-value	0.0010

Table 5.2 – P-value and Correlation Plot for Total Variance method

R	0.57
p-value	0.0010

Fig. 5.4 (c) - which suggests that 7 components are sufficient to obtain statistically significant results. Further, the dual plot showing the variation of p-value with principle components is shown in Fig. 5.5. In table 5.1 and 5.2 the correlation and p-values for the two methods considered are shown with Fig. 5.4 (b) showing the scatter plots. Its corresponding brain and behavioral saliency plots can be seen in Fig.5.8 and Fig. 5.10.

Table 5.3 – P-value and Correlation Plot for Total Variance method

R	0.57
p-value	0.050

### 5.5.2 Stable and Deteriorated Controls

In Figure 5.6(a) you can observe the cumulative increase percentage variance preserved with number of principle components. As the components were chosen based on Marchenko's pastur its plot is shown in Fig. 5.6(c) - which suggests that five components must be preserved. Further, the dual plot showing the variation of p-value with principle components is shown in Fig. 5.7. In table 5.3 and 5.2 the correlation and p-values for the two methods considered are shown with Fig. 5.4 (b) showing the scatter plot (Red-dCON, Blue-sCON). The corresponding brain and behavioral saliency plots can be visualized in Fig.5.9 and Fig. 5.11.

## 5.6 Results using TBSS - Single Behavioral Analysis

Then a similar analysis was conducted by working with each individual behavioral measure separately. During the analysis it was found that Neuroticism, Openness and Verbal Episodic Memory do not give statistically significant results and hence, their brain saliency vectors are not shown.

### 5.6.1 Stable Controls

On observing the Dual plots, for each of the 7 behavioral measures, not all but 4 give statistically significant result, when multiple value testing is performed.

## 5.6. Results using TBSS - Single Behavioral Analysis

Table 5.4 – P-value and Correlation Plot for Marchenko Pastur Based method

R	0.29
p-value	0.037

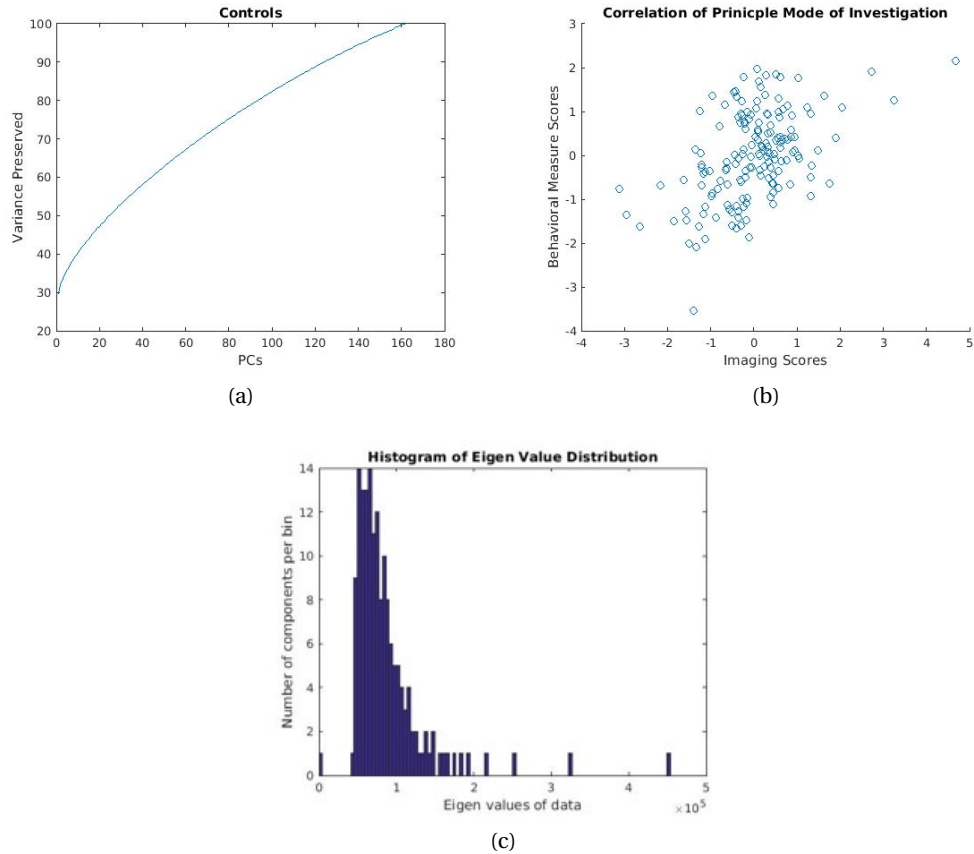


Figure 5.4 – Plots for analysis of principle components

- The ones which are statistically significant are –
  - Extraversion (Fig. 5.12)
  - Agreeableness (Fig. 5.13)
  - Conscientiousness(Fig. 5.14)
  - MMSE (Fig. 5.15)
- More details regarding the behavior of p-value Vs number of components (along with its corresponding Correlation and Varianace Preserved by them) could be obtained from the dual plot.
- The brain maps has been shown only for statistically significant behaviors using minimum number of components which correspond to 7, 7, 16 and 7 for the behaviors

## Chapter 5. Results and Discussion

---

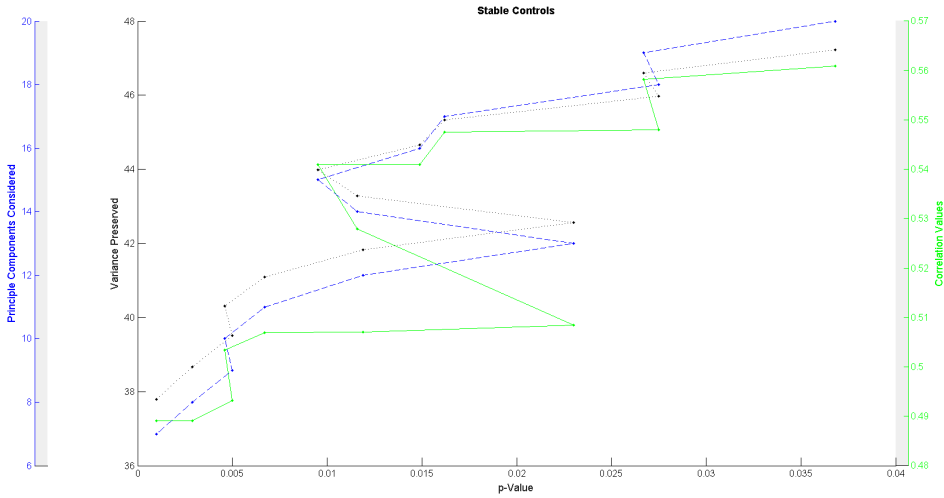


Figure 5.5 – Dual Plot - Stable Controls showing correlation, variance preserved and principle components preserved with respect to p-value

mentioned above respectively.

- To lay further emphasis on seven components – it is what Marchenko-Pasteur also suggested !!!
- The average CCA weight and its standard deviation (in brackets) of each of the aforementioned behavior on bootstrapping over 100 folds ( on Procrustes realignment).
  - $\mu = -1.0082 (\sigma = 0.0373)$
  - $-1.0011 (0.0393)$
  - $+1.0134 (0.0415)$ ; Flipped Sign in the brain map due to reference mode.
  - $-1.0545 (0.0347)$ .

### 5.6.2 Stable and Deteriorated Controls

- From the Dual plots it is evident that only 3 give statistically significant result. The ones which are statistically significant are –
  - Agreeableness (Fig. 5.16)
  - Conscientiousness (Fig. 5.18)
  - MMSE(Fig. 5.18)
- The brain maps has been shown for components corresponding to 5, 40 and 15; except the Agreeableness the number of principle components are not related to Marchenko Pastur.

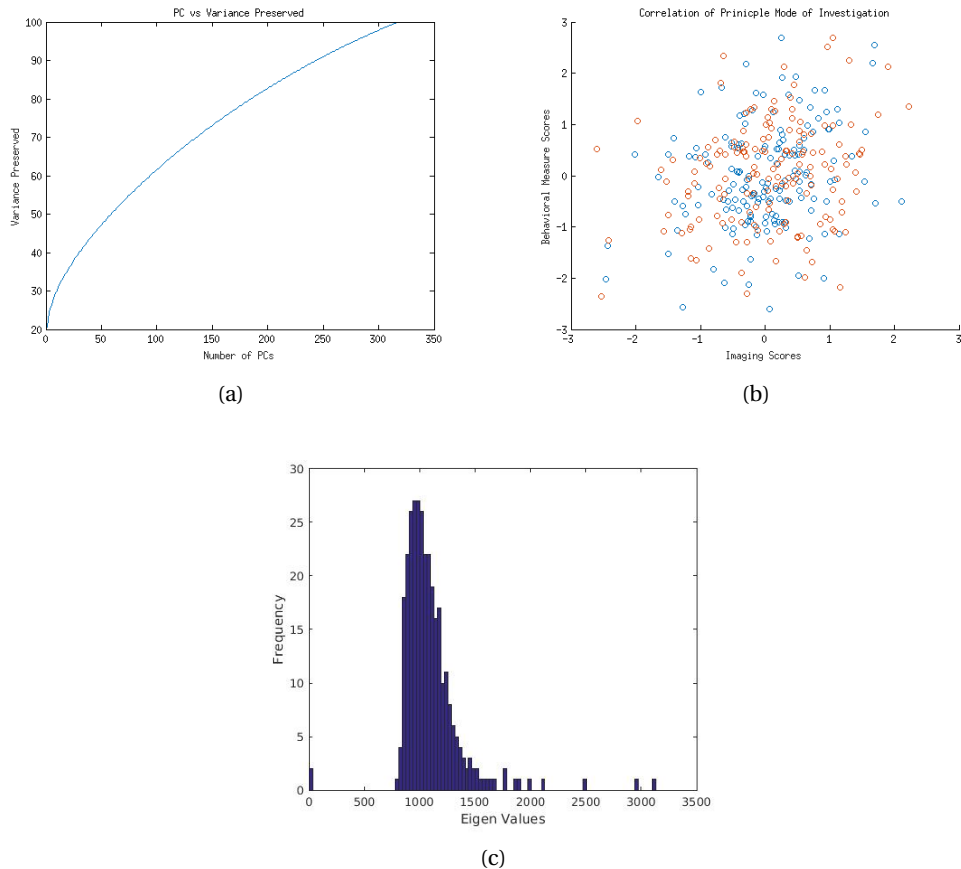


Figure 5.6 – Plots for analysis of principle components

- The average and standard deviation (in brackets) of the CCA weight are -
  - -1.0079 (0.0263).
  - 1.0078 (0.0248); Switch in sign is because of the reference mode.
  - -1.0566 (0.0274).

### 5.6.3 Interpretation using Atlas

As explained before, brain atlas is composed of serial sections along different anatomical planes of the healthy or diseased developing human brain where each relevant brain structure is assigned a number of coordinates to define its outline or volume. Since, the brain atlases are contiguous and provide comprehensive results of visual brain mapping they are overlapped with atlas to find the percentage overlap with each structure. Here, ICBM-DTI-81 Atlas was used as reference atlas and is shown in Fig. 3.1.

The Steps involved are elaborated as follows:

## Chapter 5. Results and Discussion

---

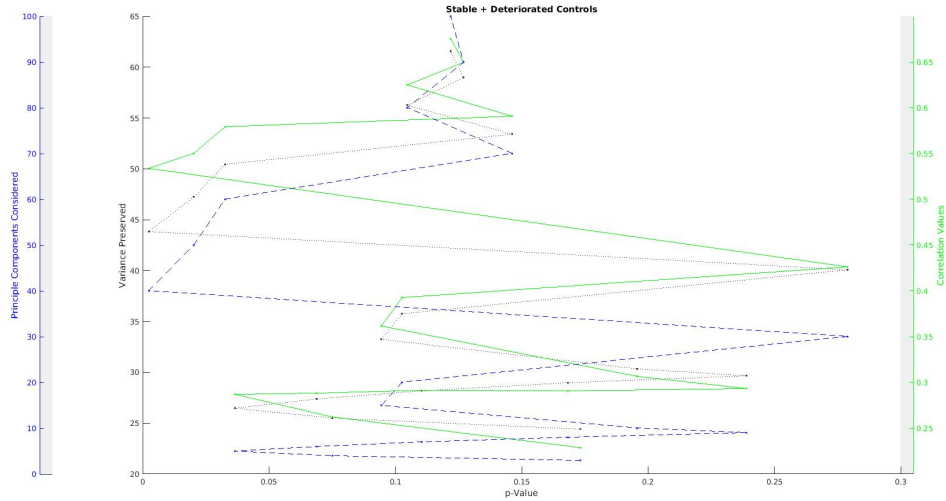


Figure 5.7 – Dual Plot - Stable and Deteriorated Controls showing correlation, variance preserved and principle components preserved with respect to p-value

- Each Structure of the Atlas ICBM-DTI-81 (total 48) was extracted separately for visualisation purpose. Then number of voxels per label was computed ( $N_a$ ).
- The Mean FA Skeleton was overlapped (voxel by voxel) with atlas and the number of overlapping voxels per atlas label ( $N_b$ ) was computed.
- The idea being that ( $N_b$ ) could serve as reference for subsequent analysis of principle components. Note - There was only 21% overlap between Mean Skeleton and Atlas on conducting the voxel by voxel analysis. The value serves as reference, as now we can theoretically expect a maximum overlap of 21% for any component, though that is never the case in practice. The reason being - A component is always a subset of the structure in its entirety.
- The components that was derived in (1) are thresholded at ( $>+2$  and  $<-2$ ) such that only voxels in this range are preserved. Note that the term component from here on refers to these filtered components.
- Then, each individual label of the atlas was overlapped separately, with all the aforementioned components and number of overlapping voxels between a component and atlas label ( $N_p$ ) was computed.
- Using the above results, we compute the percentage overlap of a given component per atlas, Relative Overlap percentage,

$$RO\% = N_a / N_b \quad (5.1)$$

## 5.6. Results using TBSS - Single Behavioral Analysis

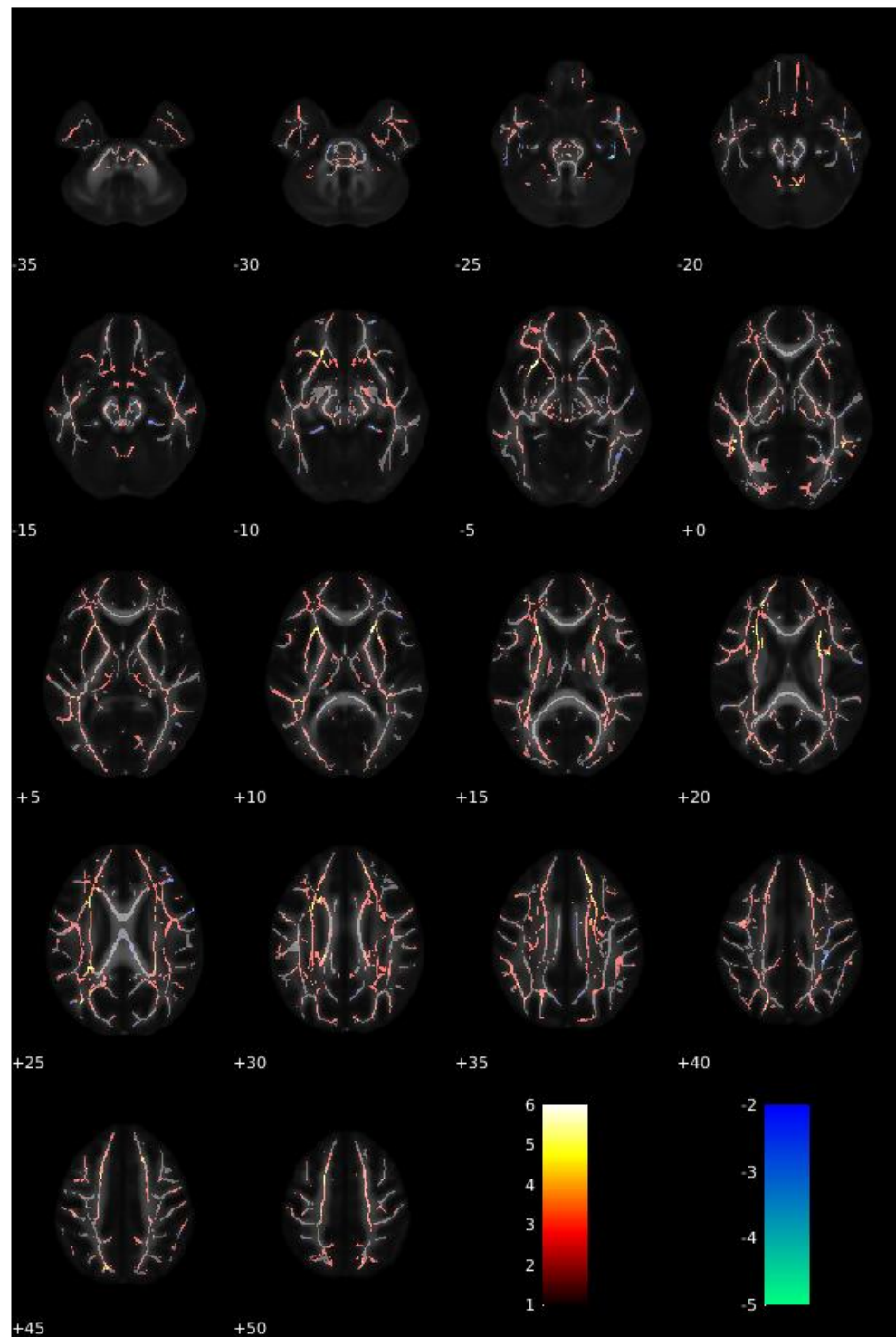


Figure 5.8 – Brain Saliency Vector for Stable Controls

## **Chapter 5. Results and Discussion**

---

Where RO% gives the percentage of overlap (in terms of voxel) of a given component with each atlas label.

This is a method that makes more sense than  $N_b/N_a$  (A novel way) as there is huge mismatch between Atlas and the TBSS Skeleton structure evident from the low overlap percentage.

### **5.7 Finding the structure in each component based on Energy**

Since, just percentage overlap in structures in terms of voxels were not that useful, the energy route was taken. The results are reported for first seven principle components (with respect to all 48 structures of the ICBM atlas) as follows:

- Percentage Energy contained in each structure for a given component and is shown in Fig. 5.19.
- Relative Percentage Energy contained which gives us the feel as to which the structure contributes the most and is shown in Fig. 5.20.
- Energy Density in which the size of the anatomical structure is taken into account as the structure size limits the amount of energy contained and is shown in Fig. 5.21.
- Effect of Laterization - to verify symmetry in the left and right hemisphere was also observed and is shown in Fig. 5.22.

This tests further proved that on thresholding only the first seven components as suggested by Marchenko Pastur are useful for analysis as they encompassed anatomical structures which have been proved to be responsible to human cognition. However, with this analysis we are able to infer more specifically as to which White Matter structure is responsible for the NEOPI Measure. The Laterization test further proved that the components preserve symmetry - a characteristic considered mandatory to draw meaningful conclusion.

## 5.7. Finding the structure in each component based on Energy

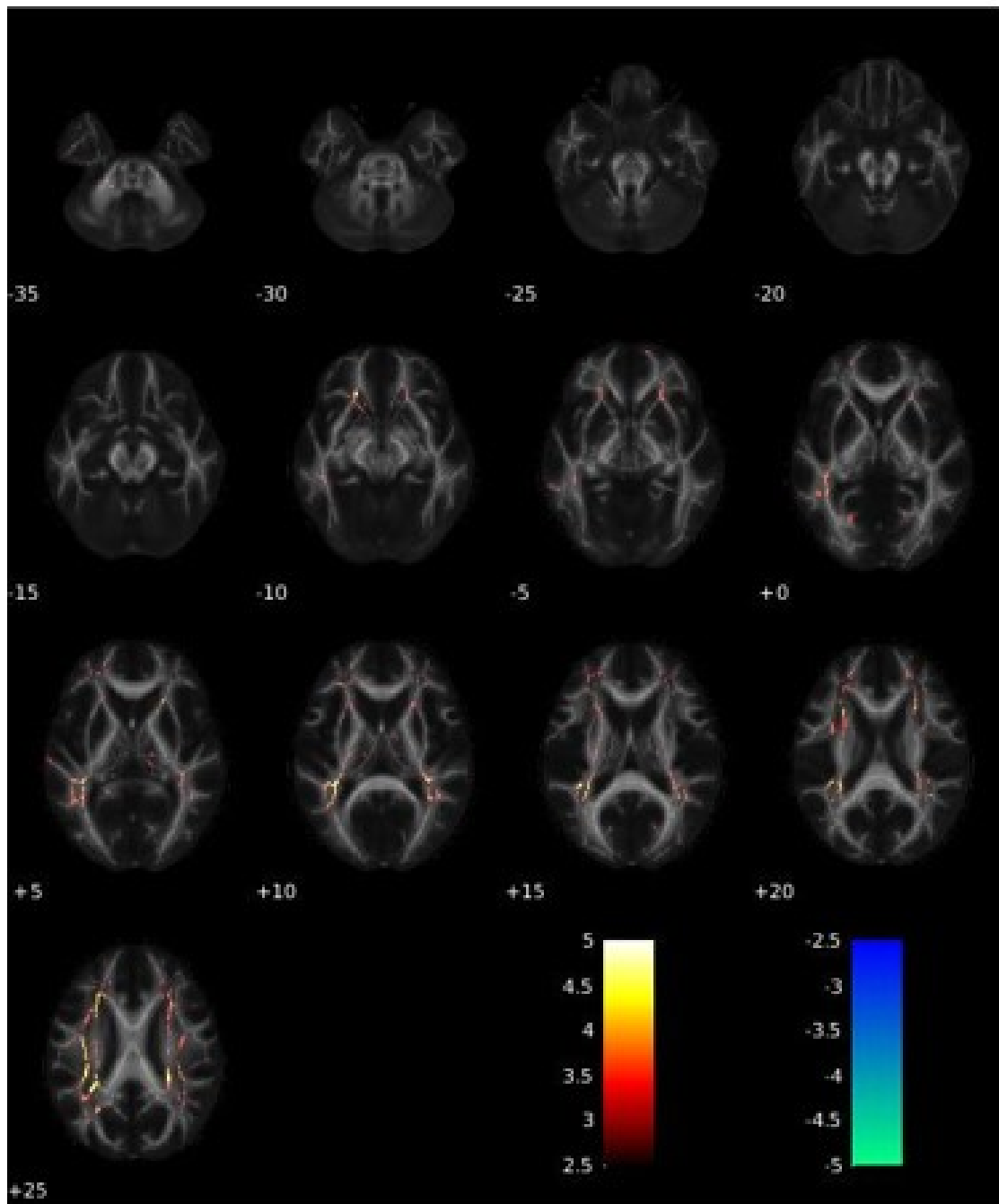


Figure 5.9 – Brain Saliency Vector for Stable and Deteriorated Controls

## Chapter 5. Results and Discussion

---

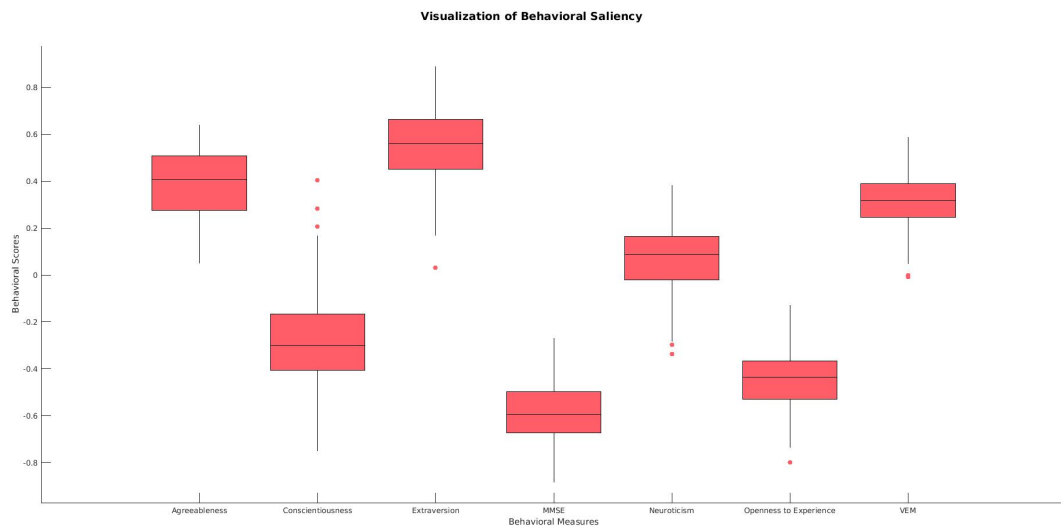


Figure 5.10 – Brain Saliency Vector for Stable Controls

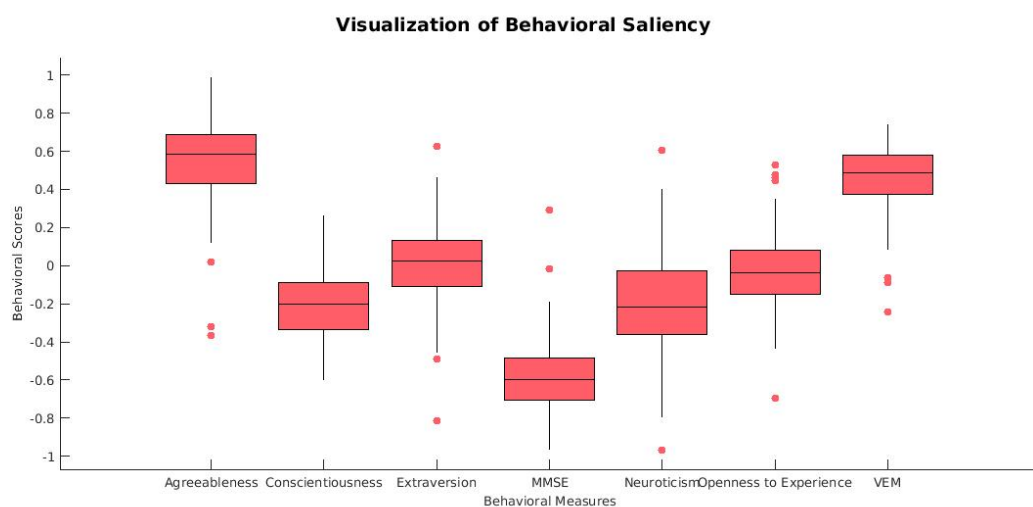


Figure 5.11 – Brain Saliency Vector for Stable and Deteriorated Controls

## **5.7. Finding the structure in each component based on Energy**

---

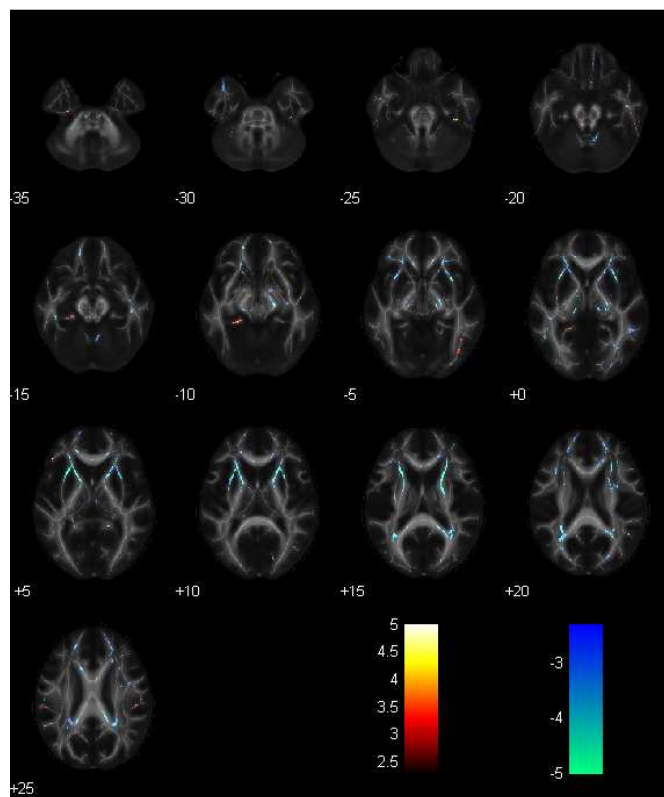


Figure 5.12 – Brain Saliency Vector for Stable Controls - Extraversion

## Chapter 5. Results and Discussion

---

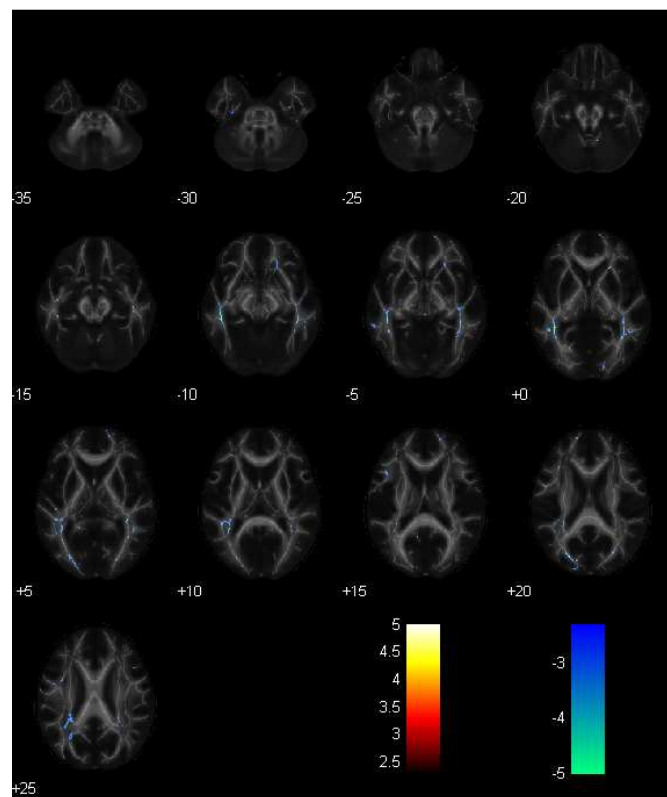


Figure 5.13 – Brain Saliency Vector for Stable Controls - Agreeableness

## **5.7. Finding the structure in each component based on Energy**

---

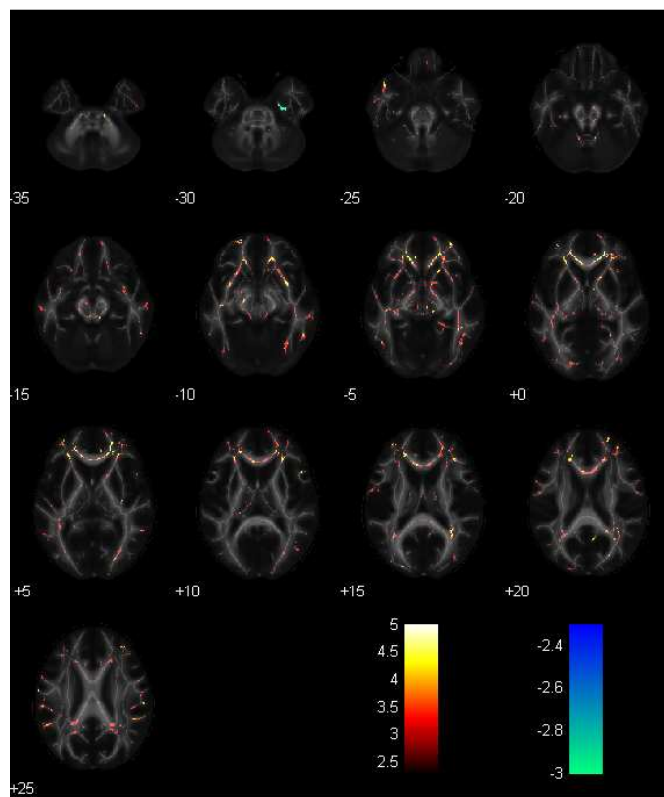


Figure 5.14 – Brain Saliency Vector for Stable Controls - Conscientiousness

## Chapter 5. Results and Discussion

---

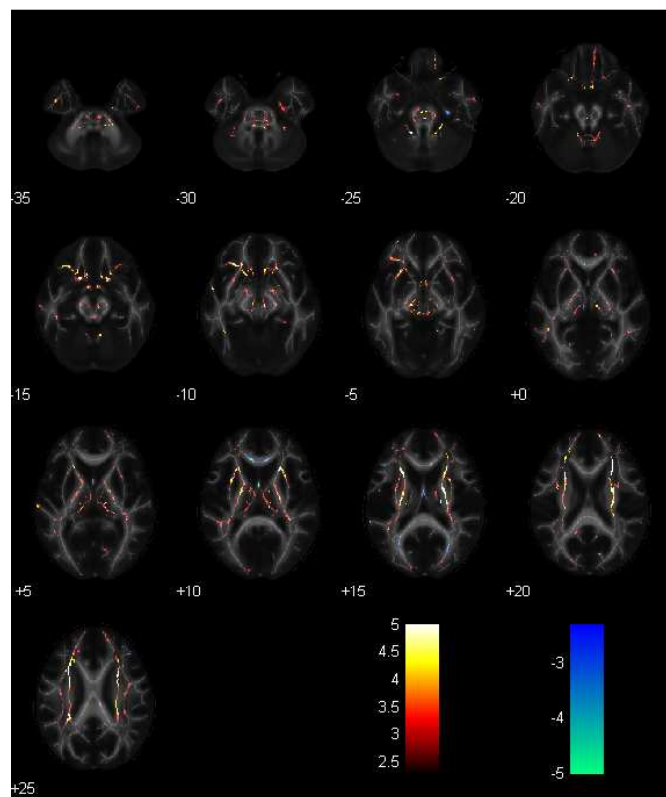


Figure 5.15 – Brain Saliency Vector for Stable Controls - MMSE

## **5.7. Finding the structure in each component based on Energy**

---

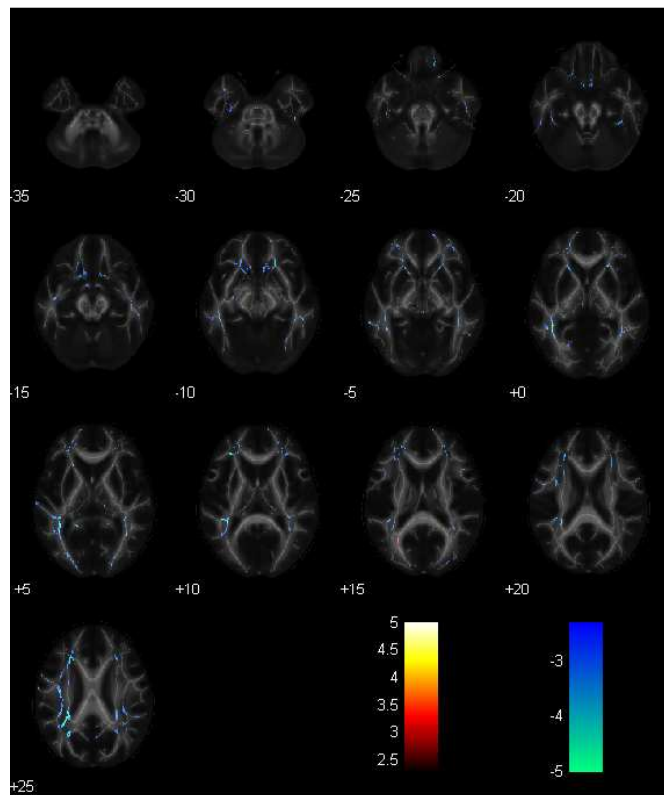


Figure 5.16 – Brain Saliency Vector for Stable and Deteriorated Controls - Agreeableness

## Chapter 5. Results and Discussion

---

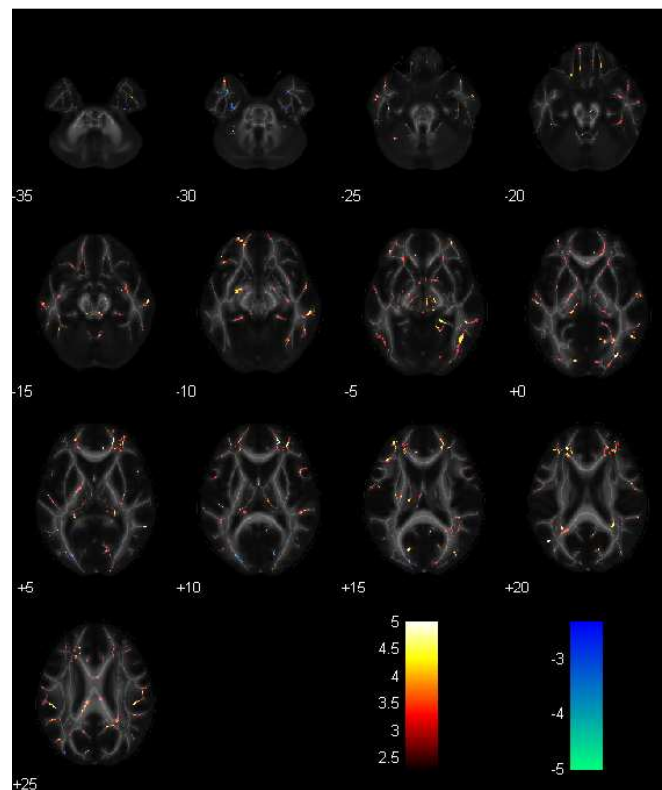


Figure 5.17 – Brain Saliency Vector for Stable and Deteriorated Controls - Conscientiousness

### **5.7. Finding the structure in each component based on Energy**

---

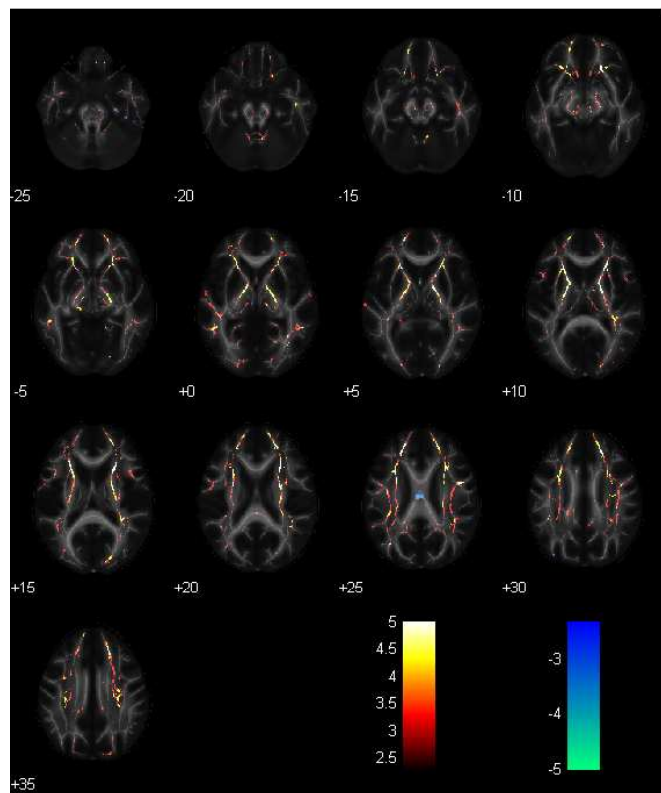


Figure 5.18 – Brain Saliency Vector for Stable and Deteriorated Controls - MMSE

## Chapter 5. Results and Discussion

---

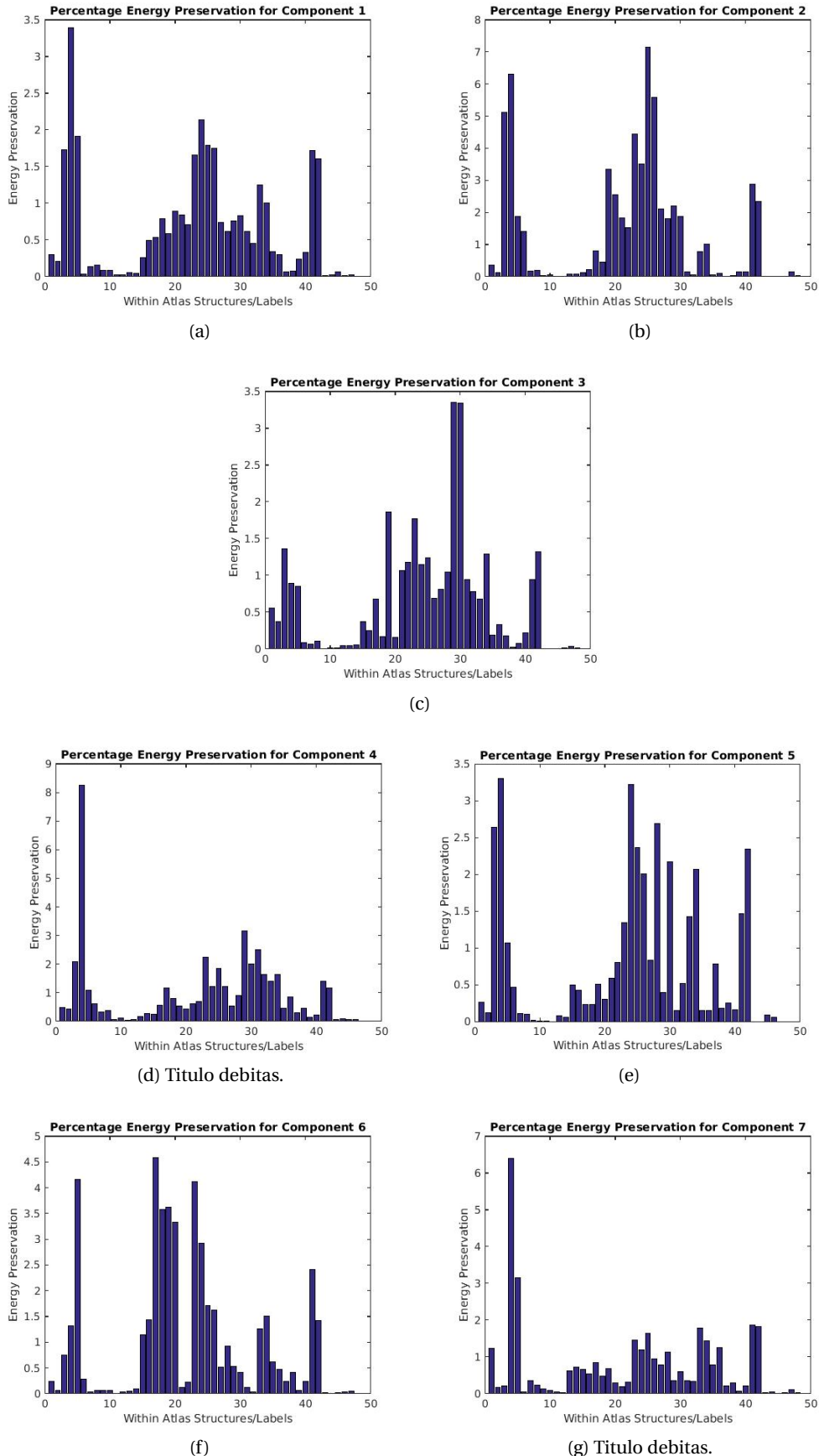


Figure 5.19 – Bar Plots showing Percentage Energy Preserved in Components 1-7 with respect to 48 atlas structures

## 5.7. Finding the structure in each component based on Energy

---

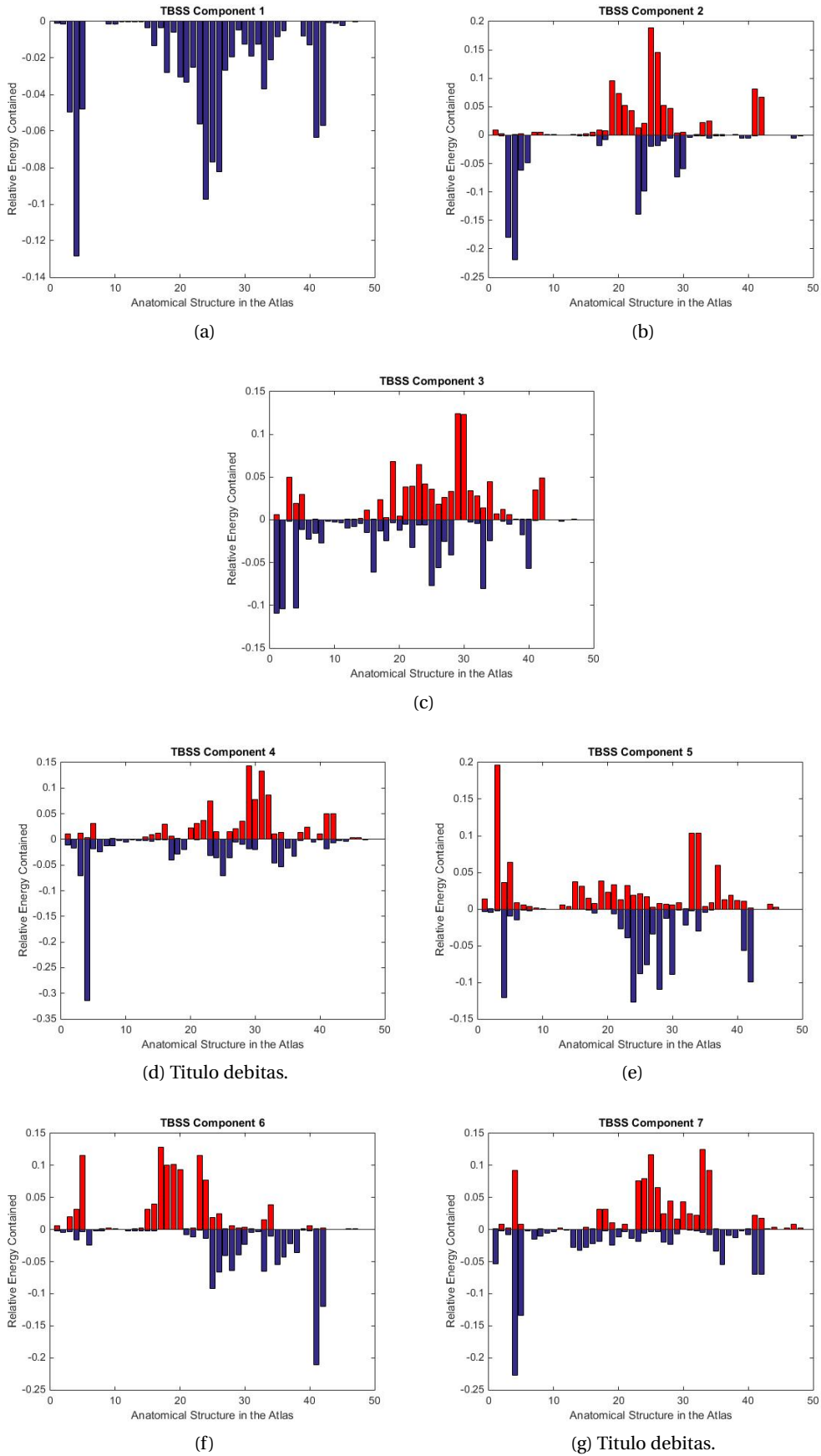


Figure 5.20 – Bar Plots showing Relative Energy Preserved in Components 1-7 with red showing percentage of positive values and blue showing percentage of negative values contained in each atlas structure

## Chapter 5. Results and Discussion

---

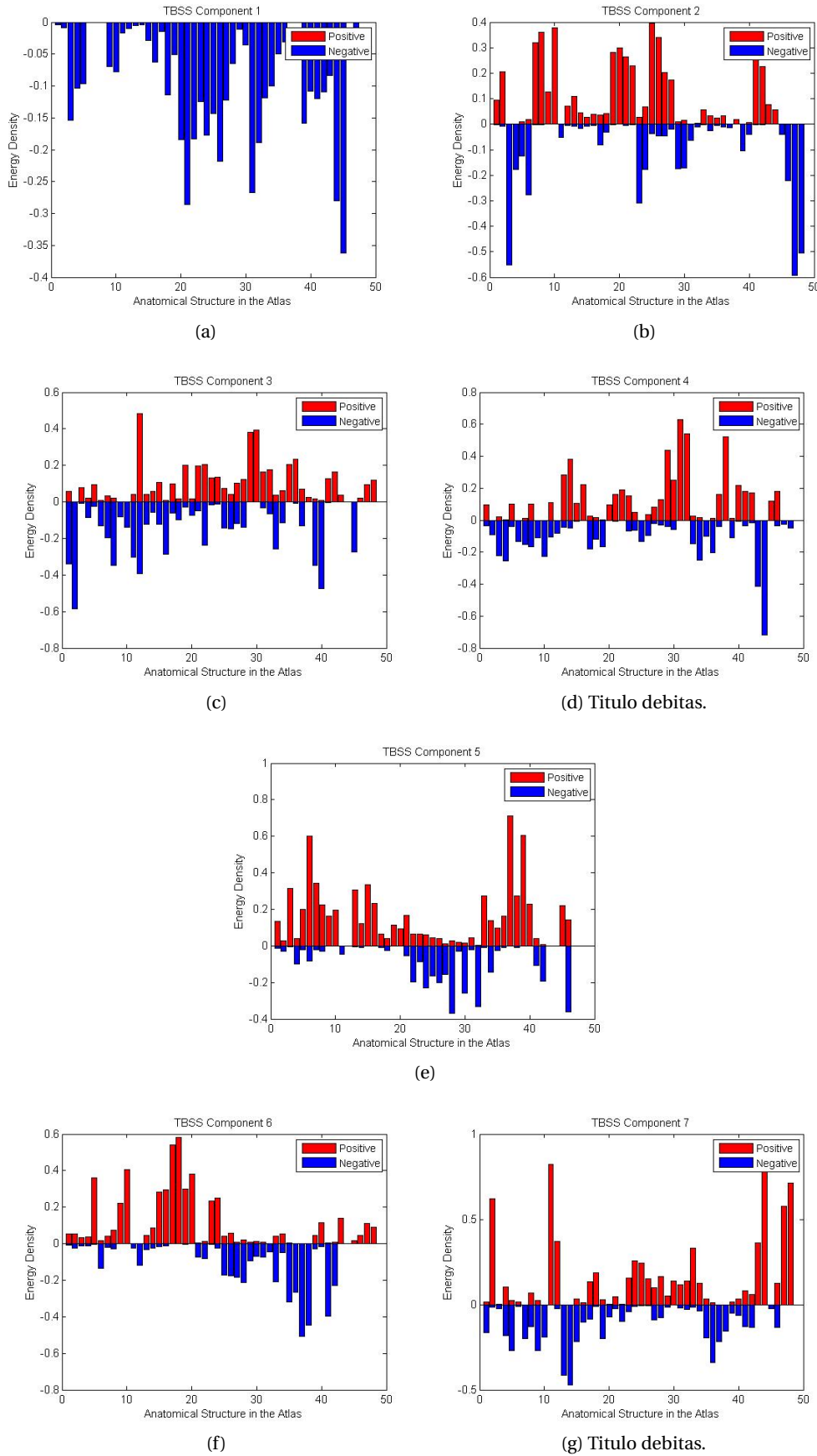


Figure 5.21 – Bar Plots showing Energy Density in Components 1-7 with red showing density of positive values and blue showing density of negative values contained in each atlas structure

## 5.7. Finding the structure in each component based on Energy

---

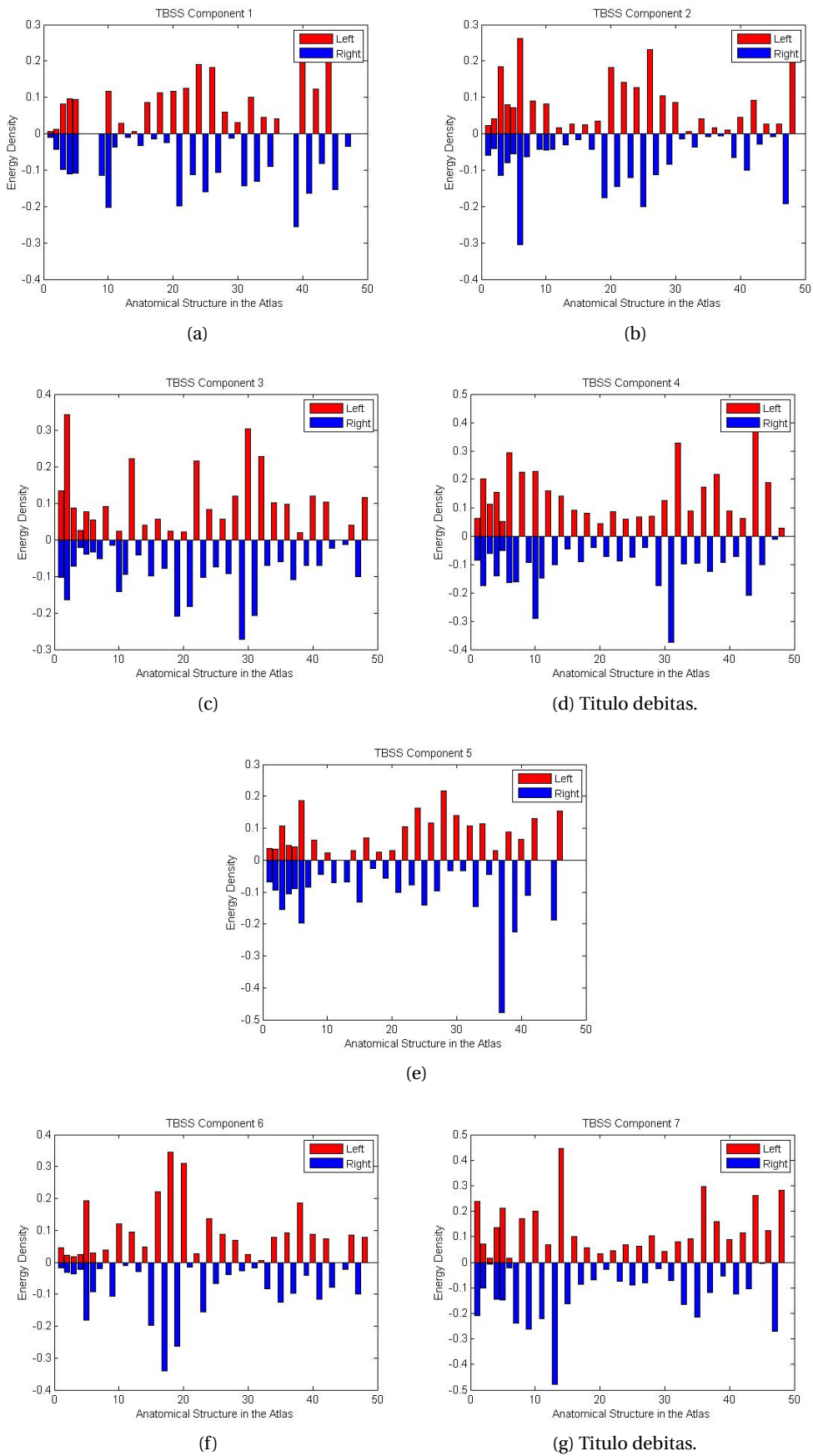


Figure 5.22 – Bar Plots showing laterization effects in Components 1-7 ith red showing left hemisphere regions and blue showing right hemisphere regions in each atlas structure



## 6 Conclusion

We started off initially investigating if a statistically significant relationship exists between 3 different brain imaging modalities namely - Arterial Spin Labelled Imaging, 3D T1 with accentuated Gray matter and Fractional Anisotropy (FA). Modalities ASL and 3DT1 failed to give statistically significant and yet meaningful results and FA was dropped though it resulted in a statistically significant result as the maps were too diffuse and were not making sense anatomically.

At this stage, TBSS was extracted from the FA data due to its improved registration for inter-subject analysis. On further investigation it was found to have a statistically significant relationship was found between structural covariance maps derived from the Tract Based Spatial Statistics Map and Neuropsychological Measure using Canonical Correlation Analysis. The results for TBSS was further divided into two sections in which both stable and deteriorated controls were examined.

- (a) A specific region of the brain responsible Combination of Behaviour.
- (b) A specific region of the brain responsible for Individual Behaviour.

However, to find specific anatomical structure analogous to structural covariance in TBSS principle components, they were overlapped with ICBM-DTI-181 Atlas. It was seen that the first 7 components had representing cut anatomical structures representing them making it possible to draw clinically viable inferences. The energy preserved in each structure was also tested along with verification of effect of laterization to further verify symmetry in the structures. The aforementioned results have been submitted to my teams Neuro-radiologist Dr. Sven Haller for further investigation - who has informed to start the manuscript preparation. During the project, a heuristic and a novel way of presenting the data were introduced - (a) Marchenko Pastur – To find components in high dimensional data; and (b) Relative Overlap percentage – A benchmark method while working with atlases. Lastly, a strong effort was put to keep the methods as simple as possible so that it reaches larger audience and get transferred into practice as soon as possible.



# Bibliography

- [Borga(2001)] Magnus Borga. Canonical correlation: a tutorial. 2001.
- [Bratislav and Sporns(2016)] Bratislav and Olaf Sporns. Network-level structure-function relationships in human neocortex. *Cerebral Cortex*, 2016.
- [Costa and McCrae(1988)] Paul T Costa and Robert R McCrae. Personality in adulthood: a six-year longitudinal study of self-reports and spouse ratings on the neo personality inventory. *Journal of personality and social psychology*, 54(5):853, 1988.
- [Efron and Tibshirani(1994)] Bradley Efron and Robert J Tibshirani. *An introduction to the bootstrap*. CRC press, 1994.
- [Jolliffe(2002)] Ian Jolliffe. *Principal component analysis*. Wiley Online Library, 2002.
- [Le Bihan(2001)] Denis Le Bihan. Diffusion tensor imaging: concepts and applications. *Journal of magnetic resonance imaging*, 13(4):534–546, 2001.
- [Matthews and Hampshire(2016)] Paul M Matthews and Adam Hampshire. Clinical concepts emerging from fmri functional connectomics. *Neuron*, 91(3):511–528, 2016.
- [McCrae and Costa(1986)] Robert R McCrae and Paul T Costa. Personality, coping, and coping effectiveness in an adult sample. *Journal of personality*, 54(2):385–404, 1986.
- [McCrae and John(1992)] Robert R McCrae and Oliver P John. An introduction to the five-factor model and its applications. *Journal of personality*, 60(2):175–215, 1992.
- [McIntosh(1999)] Anthony Randal McIntosh. Mapping cognition to the brain through neural interactions. *Memory*, 7(5-6):523–548, 1999.
- [Oishi et al.(2009)] Kenichi Oishi et al. Atlas-based whole brain white matter analysis using large deformation diffeomorphic metric mapping: application to normal elderly and alzheimer’s disease participants. *Neuroimage*, 46(2):486–499, 2009.
- [Petcharunpaisa(2010)] Petcharunpaisa. Wjr. *World*, 2(10):384–398, 2010.
- [Smith(2006)] Stephen M Smith. Tract-based spatial statistics: voxelwise analysis of multi-subject diffusion data. *Neuroimage*, 31(4):1487–1505, 2006.

## Bibliography

---

- [Smith and Nichols(2015)] Stephen M Smith and Nichols. A positive-negative mode of population covariation links brain connectivity, demographics and behavior. *Nature neuroscience*, 18(11):1565–1567, 2015.
- [Sporns(2014)] Olaf Sporns. Contributions and challenges for network models in cognitive neuroscience. *Nature neuroscience*, 17(5):652–660, 2014.
- [Tulving and Markowitsch(1998)] Endel Tulving and Hans J Markowitsch. Episodic and declarative memory: role of the hippocampus. *Hippocampus*, 8(3):198–204, 1998.